ЛЕКЦИИ 4 и 5. Пьезо- и магнитоэлектрические материалы и их биомедицинские применения

Д.т.н., профессор Сурменев Роман Анатольевич

- Piezoelectric materials

Piezoelectric and subgroup

The piezoelectric effect was discovered in 1880 by two French physicists, brothers Pierre and Paul-Jacques Curie, in crystals of quartz, tourmaline, and Rochelle salt (potassium sodium tartrate). **They took the name from the Greek work piezein, which means "to press."**

- These **32 point groups** are subdivisions of **7 basic crystal systems**:
  - ***triclinic,***
  - ***monoclinic,***
  - ***orthorhombic,***
  - ***tetragonal,***
  - ***rhombohedral (trigonal),***
  - ***hexagonal, and***
  - ***cubic.***

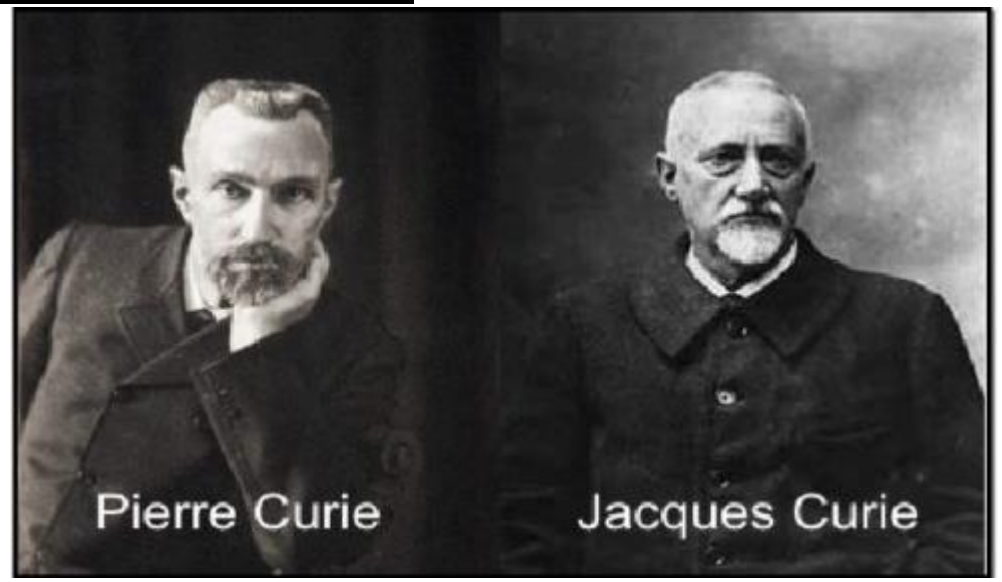

- Of the 32 point groups, 21 classes do not possess a center of symmetry (*a necessary condition for piezoelectricity to exist*) and 20 of these are piezoelectric.
- One class, although lacking a center of symmetry, is not piezoelectric because of other combined symmetry elements.

Quartz – an example

PMT-PT – an example

$(PbMg_{1/3}Nb_{2/3}O_3)_{1-x}-(PbTiO_3)_x$,
e.g. with x=0.35 (**PMN-PT** 35%)

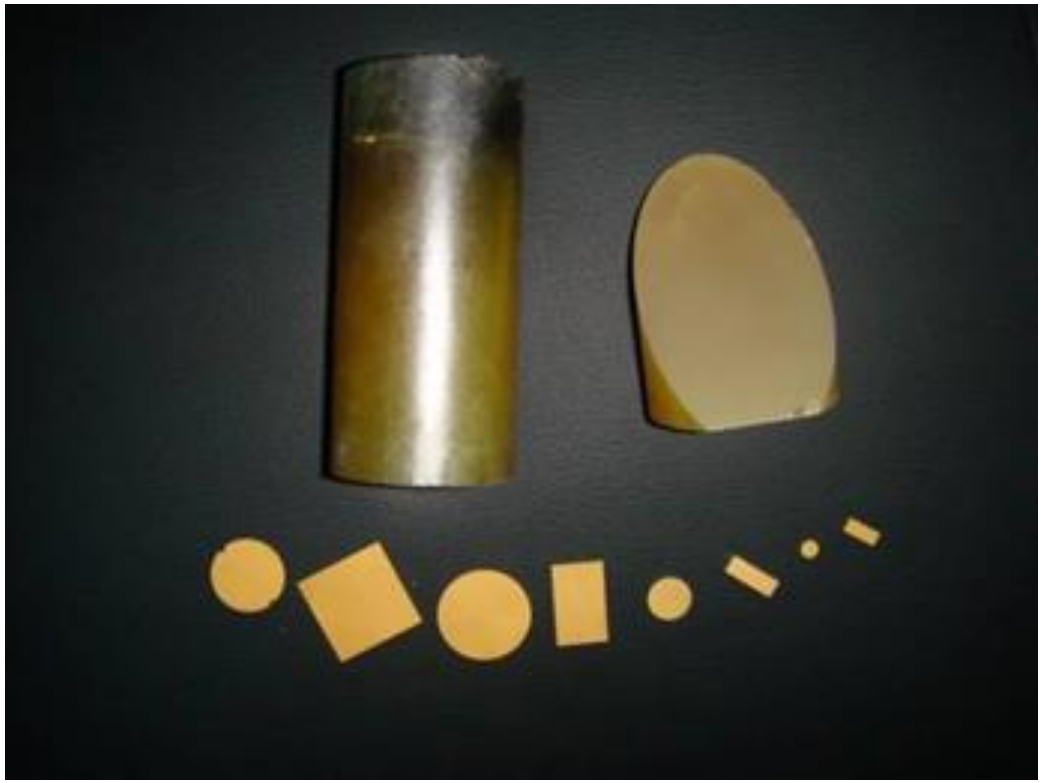

How is piezoelectric ceramic made?

- A traditional piezoelectric ceramic is ***perovskite crystal***, each consisting of a small, tetravalent metal ion, usually titanium or zirconium, in a lattice of larger, divalent metal ions, usually lead or barium, and O_2- ions.

- Under conditions that confer tetragonal or rhombohedral symmetry on the crystals, each crystal has a dipole moment.

(a) Temperature above Curie point

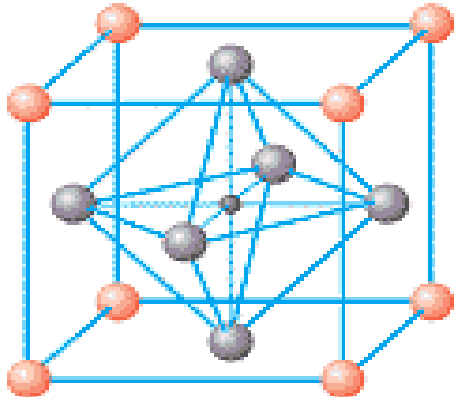

Cubic lattice, symmetric arrangement of positive and negative charges

(b) Temperature below Curie point

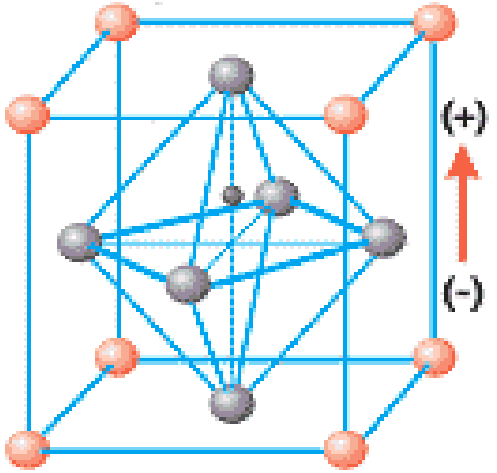

Tetragonal (orthorombic) lattice, crystal has electric dipole

A(II+) – Ba, Pb, other large divalent metal ion

O(II-) – oxygen

B(IV+) – Ti, Zr, other smaller tetravalent metal ion

Polarization of a piezoelectric material

- Above a critical temperature, ***the Curie point***, each perovskite crystal exhibits a simple cubic symmetry with no dipole moment.

(e.g. $BaTiO_3$ – 120 °C, Pb-based piezoelectric ceramics ($T_C \approx 200$ °C), PMN-PH-PT ceramics - $T_C \approx 297$ °C etc)

- At temperatures below the Curie point, however, each crystal has tetragonal or rhombohedral symmetry and a dipole moment.

(a) Temperature above Curie point

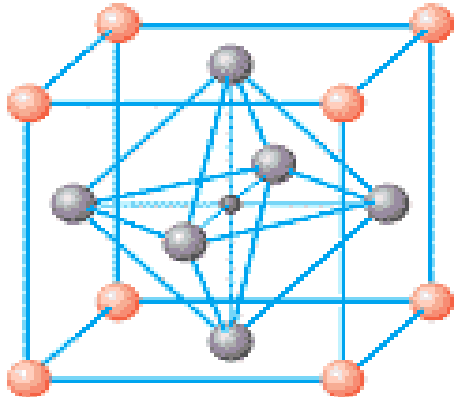

Cubic lattice, symmetric arrangement of positive and negative charges

(b) Temperature below Curie point

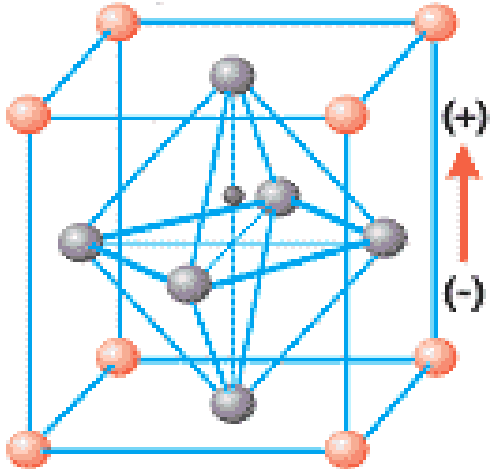

Tetragonal (orthorombic) lattice, crystal has electric dipole

A(II+) – Ba, Pb, other large divalent metal ion

O(II-) – oxygen

B(IV+) – Ti, Zr, other smaller tetravalent metal ion

https://iopscience.iop.org/article/10.1143/JJAP.34.5443; **Journal of Alloys and Compounds** Volume 735, 25 February 2018, Pages 496-509

a) random orientation of polar domains prior to polarization

b) polarization in DC electric field

c) remanent polarization after electric field removed

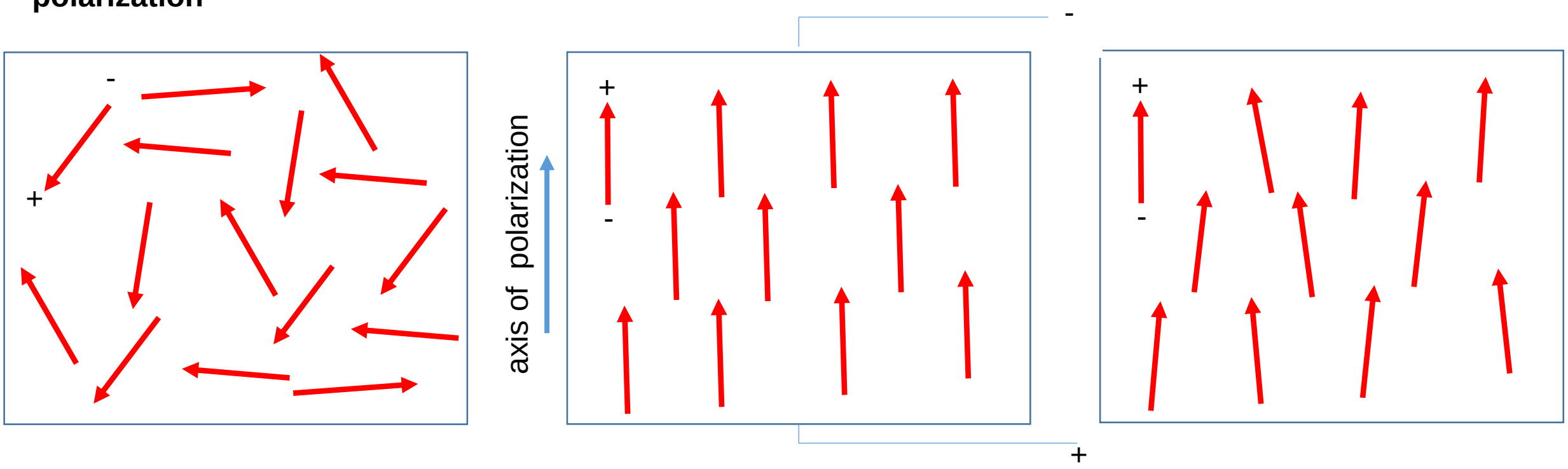

Electric dipoles in Weiss domains; (a) unpoled ferroelectric ceramic, (b) during and (c) after poling (piezoelectric ceramic)

Domain Wall Movement

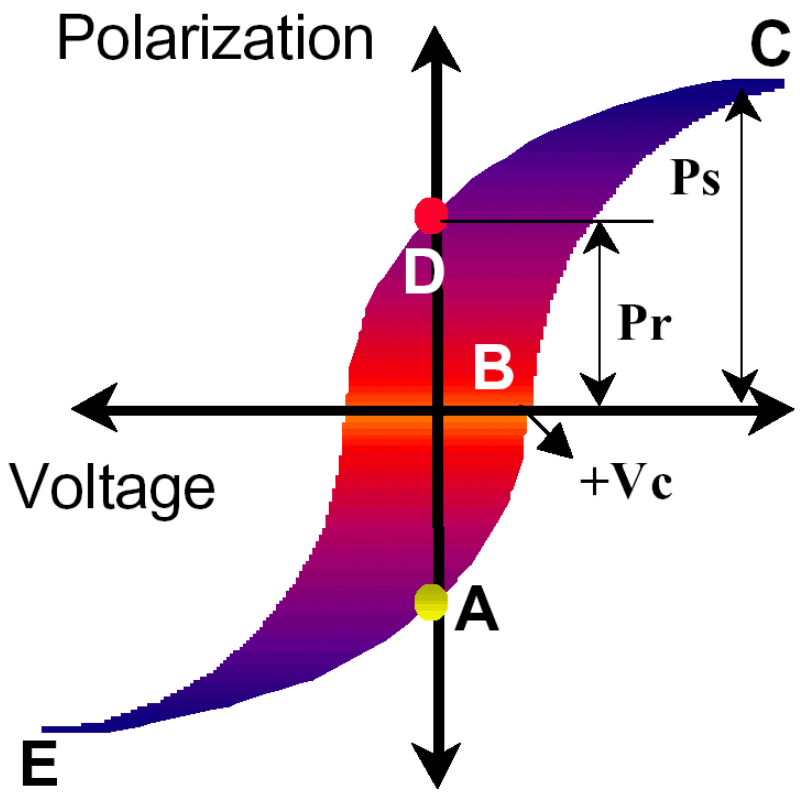

Polarization & electric field hysteresis loop

Pr – remanent polarization,
Ps – saturation polarization

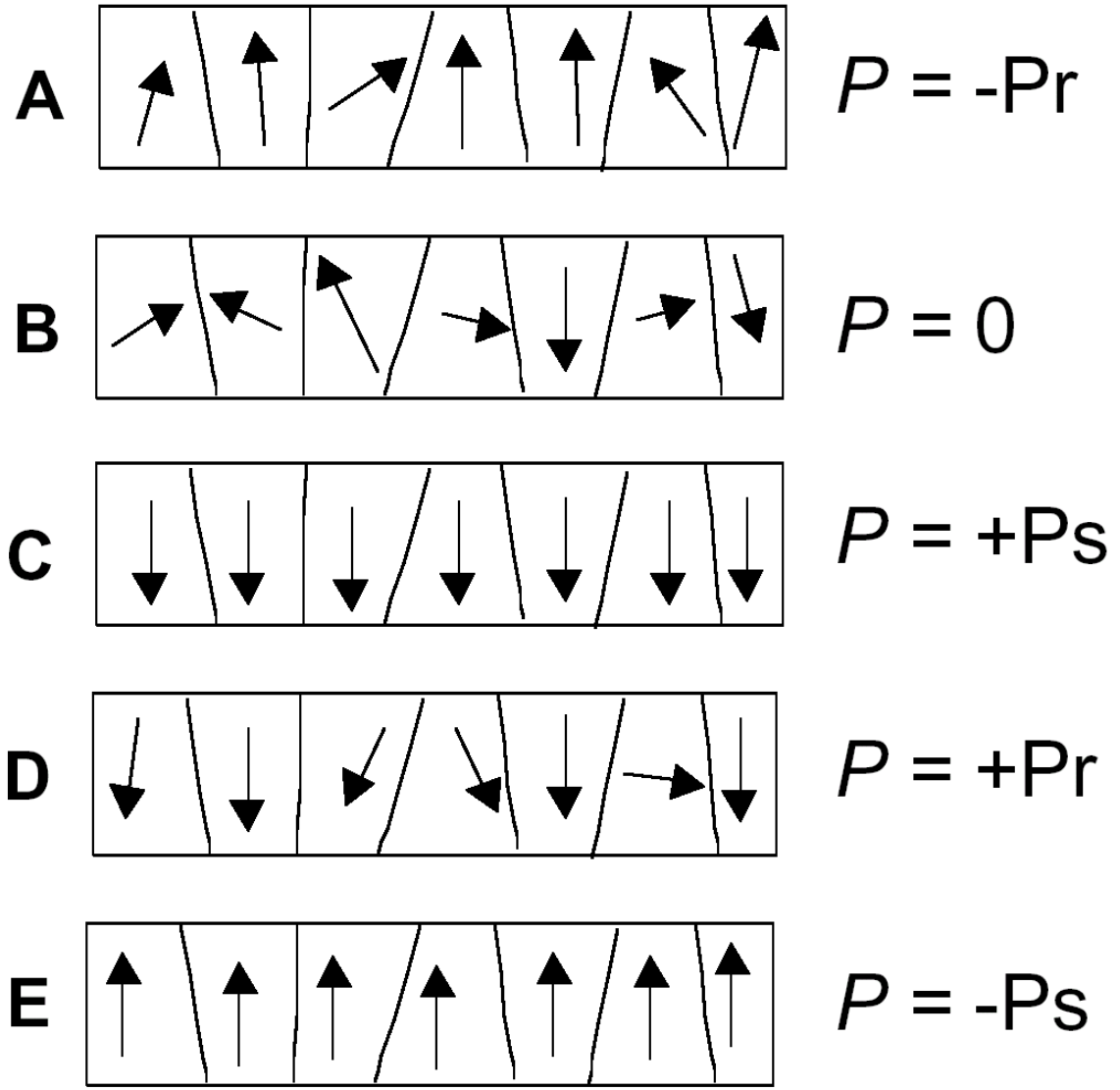

Direct piezoelectric effect

- ‘Direct’ piezoelectric effect occurs when a piezoelectric material becomes electrically charged when subjected to a mechanical stress.
- These devices can be used to detect strain, movement, force, pressure or vibration by developing appropriate electrical responses, as in the case of force and acoustic or ultrasound sensors.

Converse piezoelectric effect

- ‘Converse’ piezoelectric effect occurs when a piezoelectric material becomes strained when placed in an electric field.
- This property can be used to generate strain, movement, force, pressure or vibration through the application of suitable electric field.

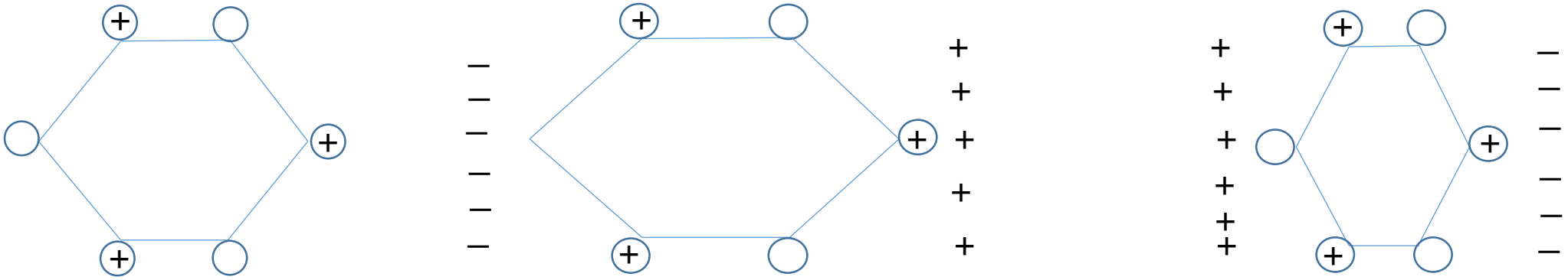

Trigonal cell unit

Piezoelectric materials are characterized by several coefficients

- **d_{ij}: Strain coefficients [m/V]:** strain developed (m/m) per electric field applied (V/m) **or** (due to the sensor / actuator properties of a piezomaterial)**.**
  Charge output coefficients [C/N]: charge density developed (C/m^2) per given stress (N/m^2).

- **g_{ij}: Voltage coefficients or field output coefficients [Vm/N]:** open circuit electric field developed (V/m) per applied mechanical stress (N/m^2) **or** (due to the sensor / actuator properties of a piezomaterial) strain developed (m/m) per applied charge density (C/m^2).

- **k_{ij}: Coupling coefficients [no Dimensions].**

  The coefficients are energy ratios describing the conversion from mechanical to electrical energy or vice versa. k^2 is the ratio of energy stored (mechanical or electrical) to energy (mechanical or electrical) applied.

  Other important parameters are the Young's modulus (*describing the elastic properties of the material*) and the dielectric constant (*describing the capacitance of the material*).

3D expression

- General expression
  - Piezoelectric effect is orientation dependant
  - 1-D ➔ 3-D

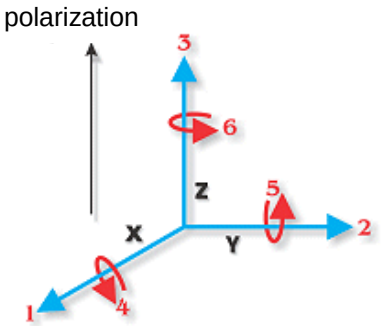

$$P_i = \sum_{k=1}^{6} d_{ik}\sigma_k$$ (E=0, no E-field)

i: 1,2,3 ➔ axial stress, 4,5,6 ➔ shear stress

$\sigma_1 = \sigma_x$, ...

$$\begin{bmatrix} P_1 \\ P_2 \\ P_3 \end{bmatrix} = \begin{bmatrix} d_{11} & d_{12} & d_{13} & d_{14} & d_{15} & d_{16} \\ d_{21} & d_{22} & d_{23} & d_{24} & d_{25} & d_{26} \\ d_{31} & d_{32} & d_{33} & d_{34} & d_{35} & d_{36} \end{bmatrix} \begin{bmatrix} \sigma_1 \\ \sigma_2 \\ \sigma_3 \\ \sigma_4 \\ \sigma_5 \\ \sigma_6 \end{bmatrix}$$

polarization

stress

$$\varepsilon_k = \sum_{i=1}^{3} \tilde{d}_{ik} E_i$$ (σ=0, no stress)

$$\begin{bmatrix} \varepsilon_1 \\ \varepsilon_2 \\ \varepsilon_3 \\ \varepsilon_4 \\ \varepsilon_5 \\ \varepsilon_6 \end{bmatrix} = \begin{bmatrix} d_{11} & d_{21} & d_{31} \\ d_{12} & d_{22} & d_{32} \\ d_{13} & d_{23} & d_{33} \\ d_{14} & d_{24} & d_{34} \\ d_{15} & d_{25} & d_{35} \\ d_{16} & d_{26} & d_{36} \end{bmatrix} \begin{bmatrix} E_1 \\ E_2 \\ E_3 \end{bmatrix}$$

strain

Field

Courtesy: http://www.pitt.edu

Piezoelectric coefficients

For Piezoelectric PZT, $BaTiO_3$, $PbTiO_3$

(E=0, no E-field)

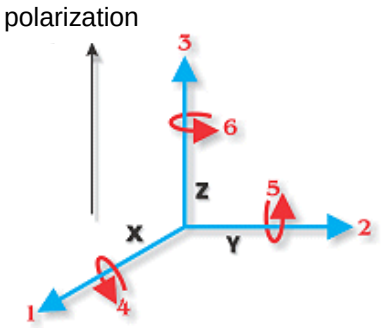

$$P_i = \sum_{k=1}^{6} d_{ik}\sigma_k$$

$$\begin{bmatrix} P_1 \\ P_2 \\ P_3 \end{bmatrix} = \begin{bmatrix} 0 & 0 & 0 & 0 & d_{15} & 0 \\ 0 & 0 & 0 & d_{15} & 0 & 0 \\ d_{31} & d_{31} & d_{33} & 0 & 0 & 0 \end{bmatrix} \begin{bmatrix} \sigma_1 \\ \sigma_2 \\ \sigma_3 \\ \sigma_4 \\ \sigma_5 \\ \sigma_6 \end{bmatrix}$$

(σ=0, no stress)

$$\varepsilon_k = \sum_{i=1}^{3} \tilde{d}_{ik} E_i$$

$$\begin{bmatrix} \varepsilon_1 \\ \varepsilon_2 \\ \varepsilon_3 \\ \varepsilon_4 \\ \varepsilon_5 \\ \varepsilon_6 \end{bmatrix} = \begin{bmatrix} 0 & 0 & d_{31} \\ 0 & 0 & d_{31} \\ 0 & 0 & d_{33} \\ 0 & d_{15} & 0 \\ d_{15} & 0 & 0 \\ 0 & 0 & 0 \end{bmatrix} \begin{bmatrix} E_1 \\ E_2 \\ E_3 \end{bmatrix}$$

Courtesy: http://www.pitt.edu

Piezoelectric coefficients (continued)

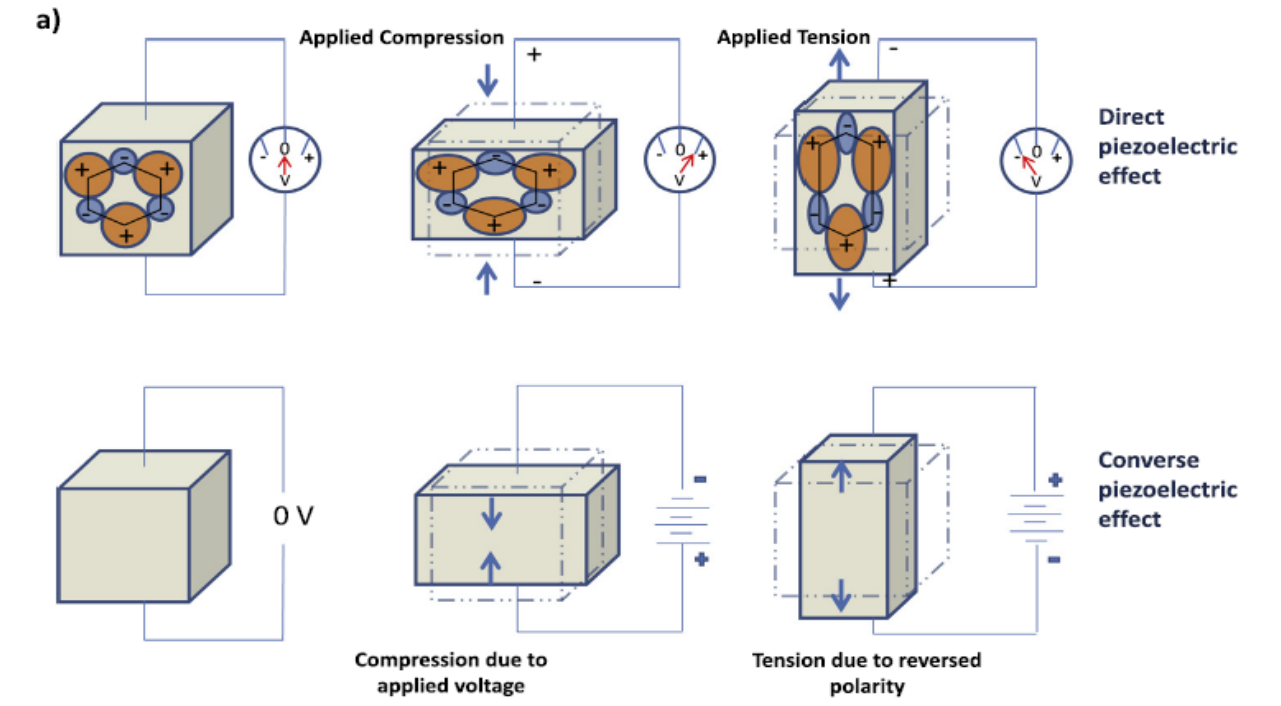

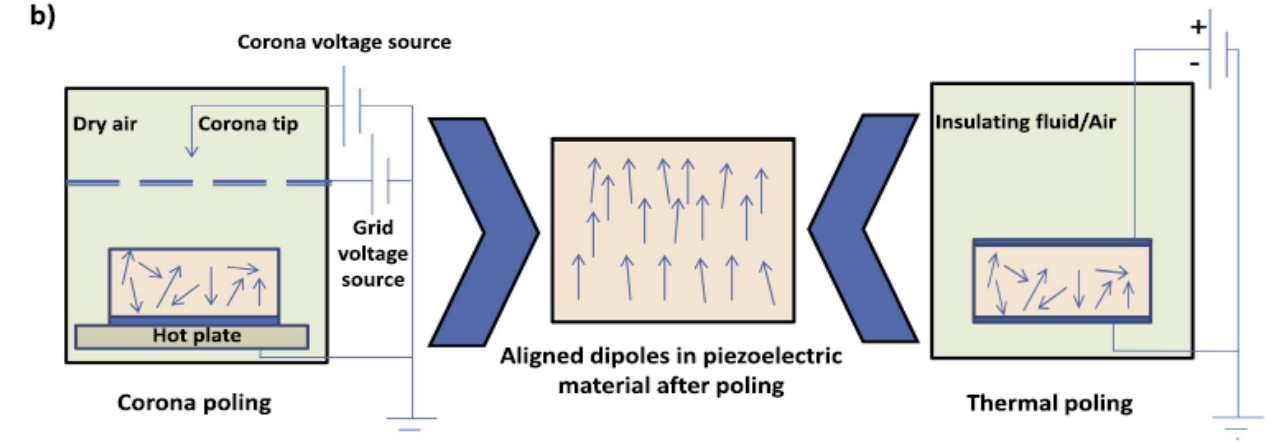

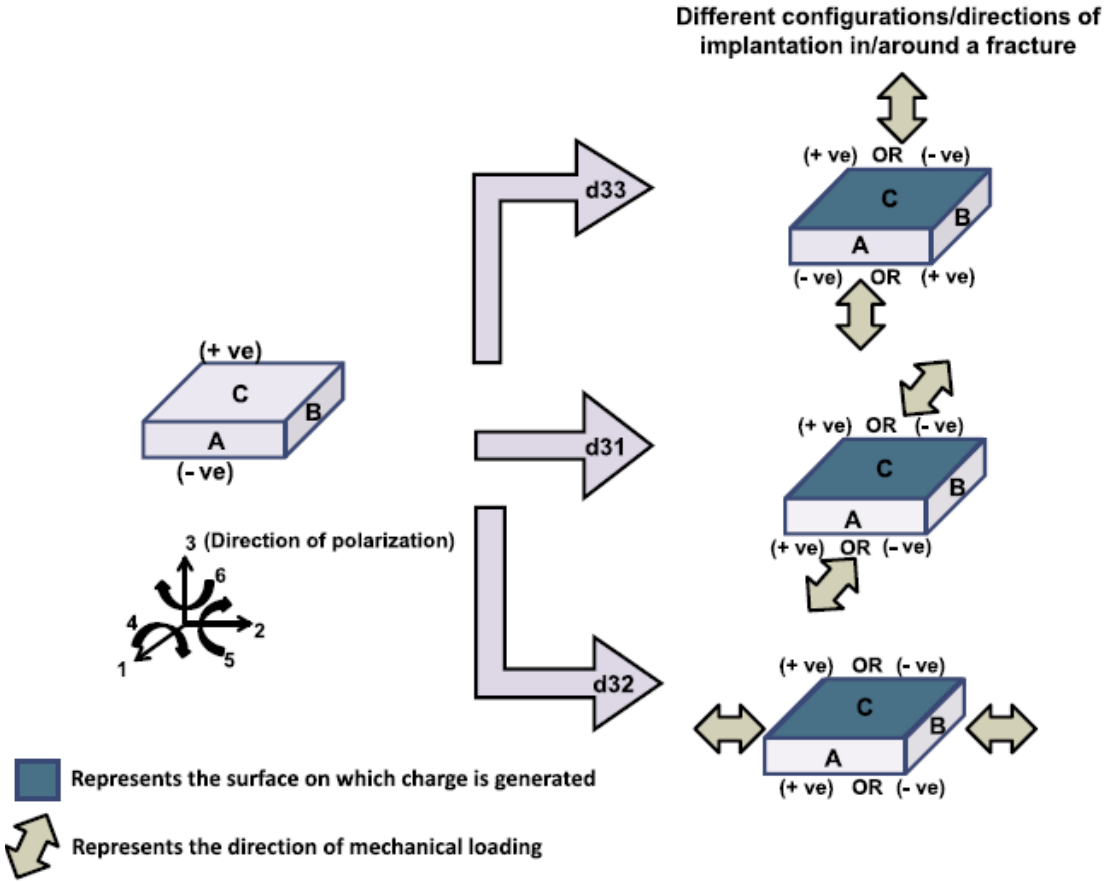

- To link electrical and mechanical quantities double subscripts (i.e. d_{ij}) are introduced.
- The first subscript gives the ***direction of the excitation***, and
- The second describes the ***direction of the system response***.

B. Tandon, et al, Acta Biomateriala, 2018

- In the −33 mode, a force is applied in the same direction as the poling direction, such as the compression of a piezoelectric block that is poled on its top and bottom surfaces.

- d_{33} applies when the electric field is along the polarization axis (direction 3) and the strain (deflection) is along the same axis.

- **Conventionally**, the −31 mode has been the most commonly used coupling mode: however, the −31 mode yields a lower coupling coefficient, *k*, than the −33 mode.

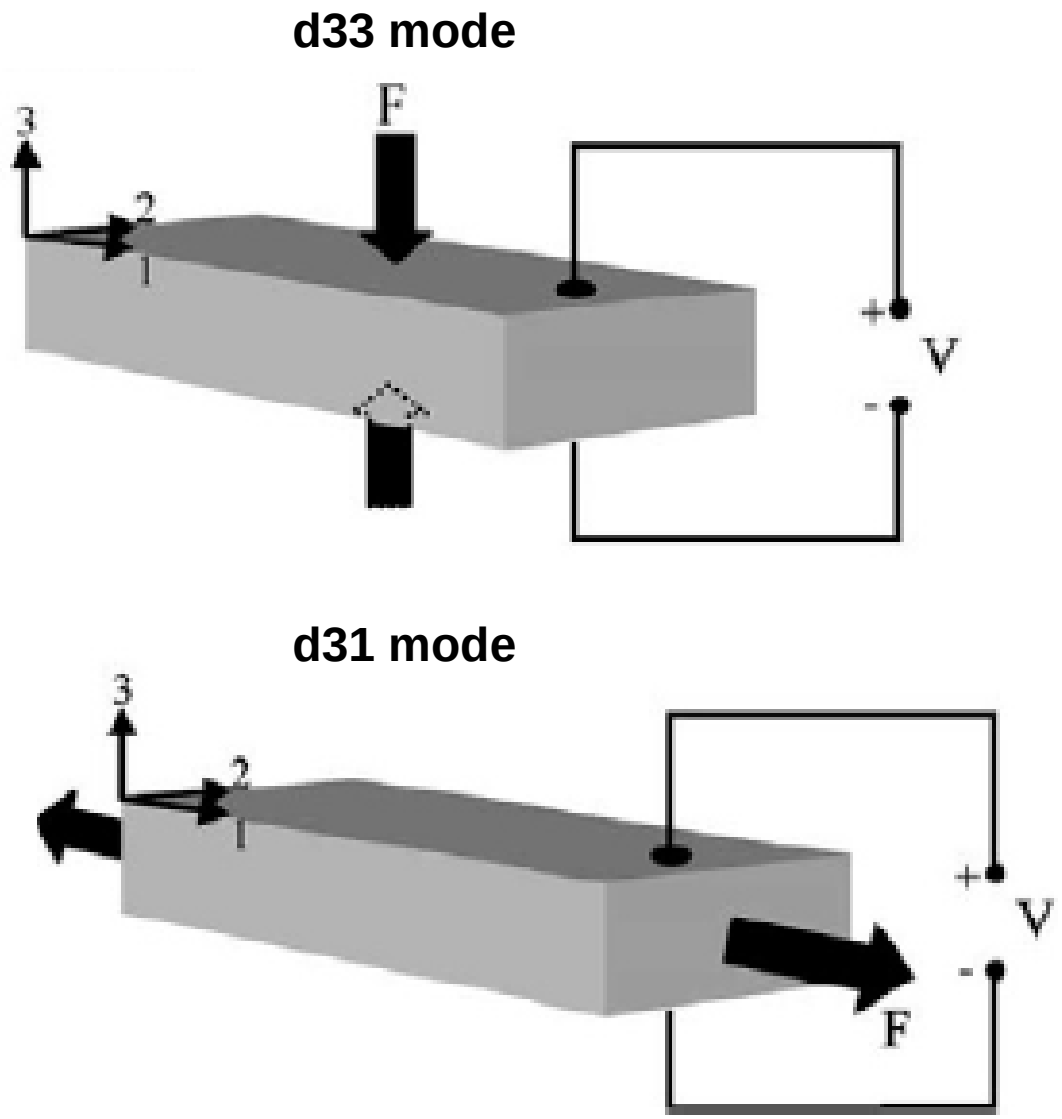

Illustration of −33 mode and −31 mode operation for piezoelectric materials. (Figure from Roundy *et al* 2003, © 2003, Elsevier.)

Smart. Mater. Struct. 16 (2007) R1-R21

Energy harvesting performance of a piezoelectric generator

$$I_{sc} = \frac{Q}{\Delta t} = \frac{d_{33} \cdot \Delta F}{\Delta t} = d_{33} \cdot A \cdot \sigma \cdot Y$$

$$V_{oc} = \frac{Q}{C} = \left(\frac{d_{33}}{\varepsilon_0 \cdot \varepsilon_r}\right) \cdot \sigma \cdot Y \cdot h = \left(\frac{d_{33}}{\varepsilon_0 \cdot \varepsilon_r}\right) \cdot h \cdot \frac{\Delta F}{A} = g_{33} \cdot h \cdot \Delta p$$

$$V_{oc} = \left(\frac{d_{31}}{\varepsilon_0 \cdot \varepsilon_r}\right) \cdot h \cdot Y \cdot \sigma = \left(\frac{d_{31}}{\varepsilon_0 \cdot \varepsilon_r}\right) \cdot h \cdot Y \cdot \frac{\Delta l}{l} = \left(\frac{d_{31}}{\varepsilon_0 \cdot \varepsilon_r}\right) \cdot h \cdot \frac{\Delta F}{A}$$

$$U_e = \frac{1}{2} \cdot C \cdot V^2 \qquad U_e = \frac{1}{2} \cdot \frac{\varepsilon_0 \cdot \varepsilon_r \cdot A}{d} \cdot V^2 = \frac{1}{2 \cdot \varepsilon_0 \cdot \varepsilon_r} \cdot \frac{h}{A} \cdot d_{33}^2 \cdot F^2$$

$$P = \frac{V}{R_L} = V \cdot I \qquad P_D = \frac{P}{A \cdot h} = \frac{V \cdot I}{A \cdot h}$$

ZnO (sputtered thin films, **d33=246 pC/N**)

PZT (lead zirconate titanate, ceramic bulk or sputtered thin film, **d33=110 pC/N**)

Quartz (bulk single crystal, **d33=2.33 pC/N**)

PVDF (**d33=1.59 pC/N**)

where Q is charge, C is capacity, h is thickness, A is surface area, Y is Young's modulus, σ is the perpendicular strain acting on the piezoelectric material, $\Delta F/\Delta t$ is the change in force applied in the compression of the PENGs, ε_0 is the permittivity of free space, ε_r is the relative dielectric constant of the piezoelectric material, Δp is the change in pressure applied to the surface of the PENGs/PEMGs, and d_{33} is the piezoelectric charge coefficient, given in $pC \cdot N^{-1}$. The piezoelectric voltage coefficient, g_{33}, is defined as $d_{33}/\varepsilon_0\varepsilon_r$ and expressed in $mV \cdot m \cdot N^{-1}$

Surmenev, Chernozem, Surmeneva et al, Nano Energy, 2019

- Prospective biomedical applications of piezoelectric materials

Electrical activity in the human body

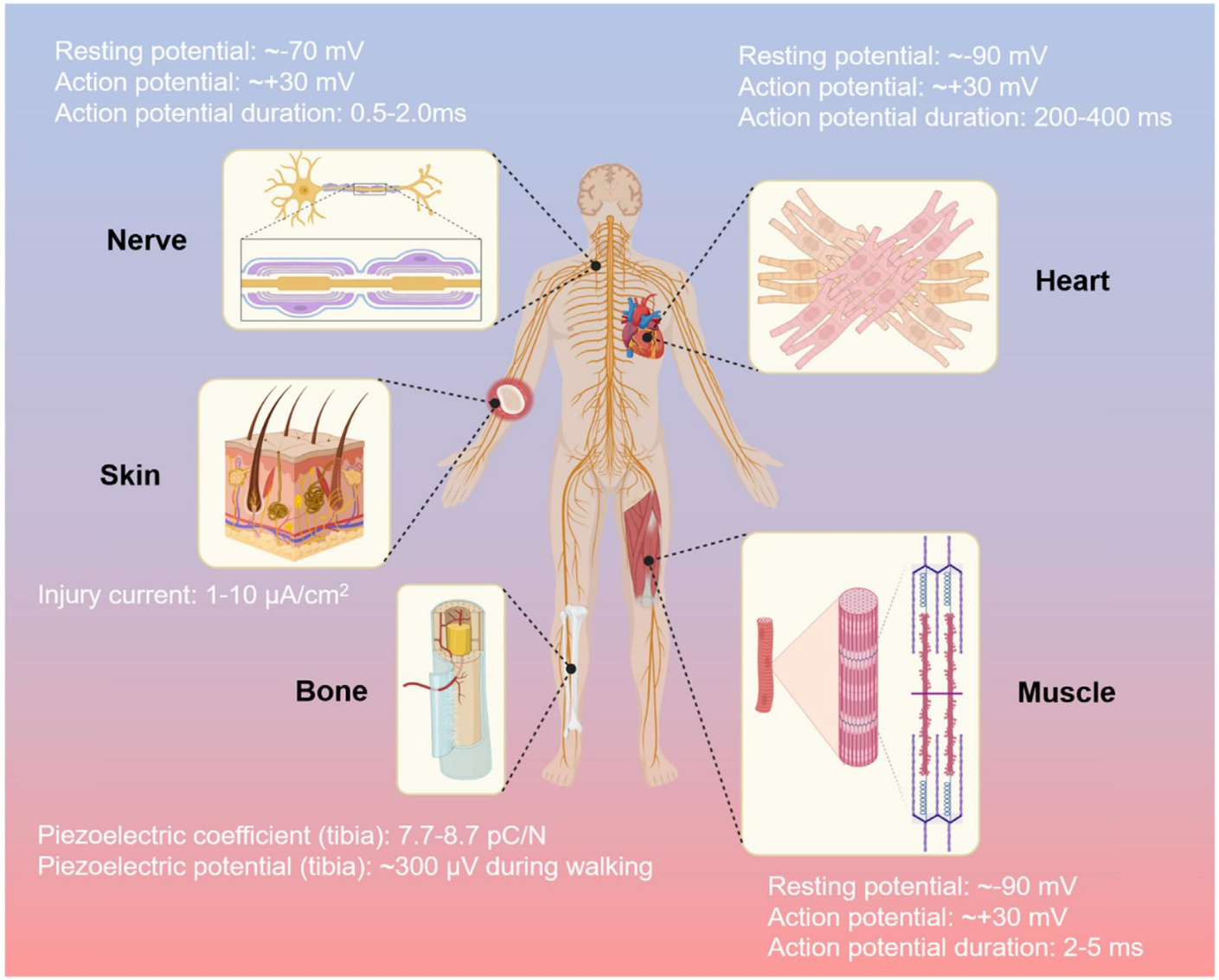

Zhang X., Li L., Ouyang J., Zhang L., Xue J., Zhang H., Tao W. Electroactive electrospun nanofibers for tissue engineering // Nano Today. 2021. Vol. 39. P. 101196

Scheme of the electrospinning process

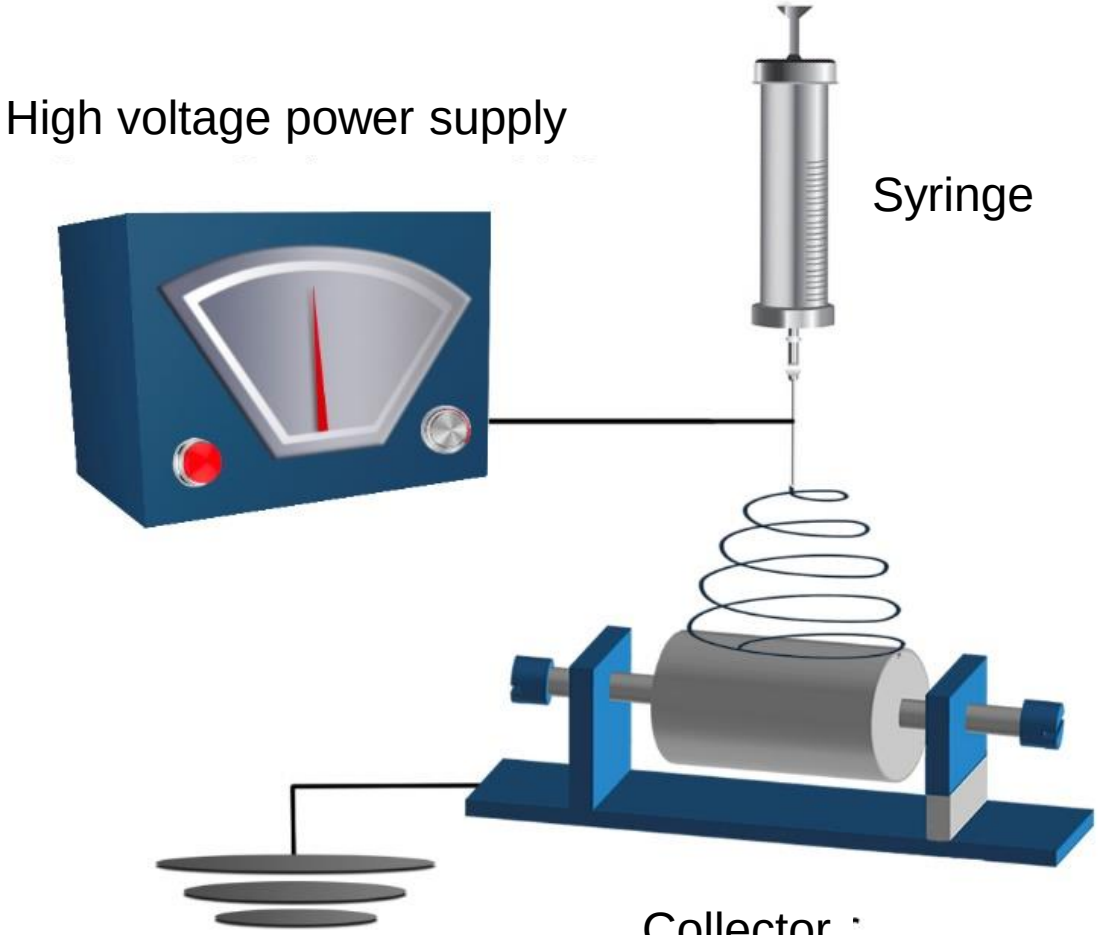

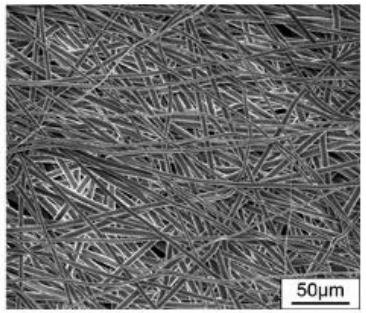

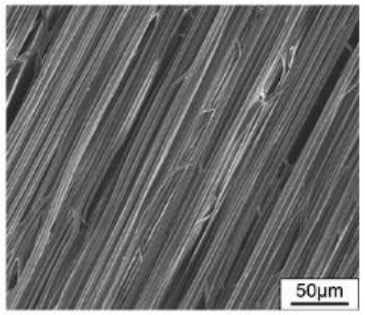

Available fiber orientation

Electrospinning technique:

- Relatively low cost of electrospinning setup;
- The usage of a wide variety of polymers and materials;
- Ease of material combination;
- Ease of fiber deposition onto other substrates;
- Production of fibers with different size (from nano to micro size) and fiber orientation.

- Poly-3-hydroxybutyrate scaffolds
- PVDF scaffolds
- PVDF-TrFE scaffolds

PVDF and PVDF-TrFE composites

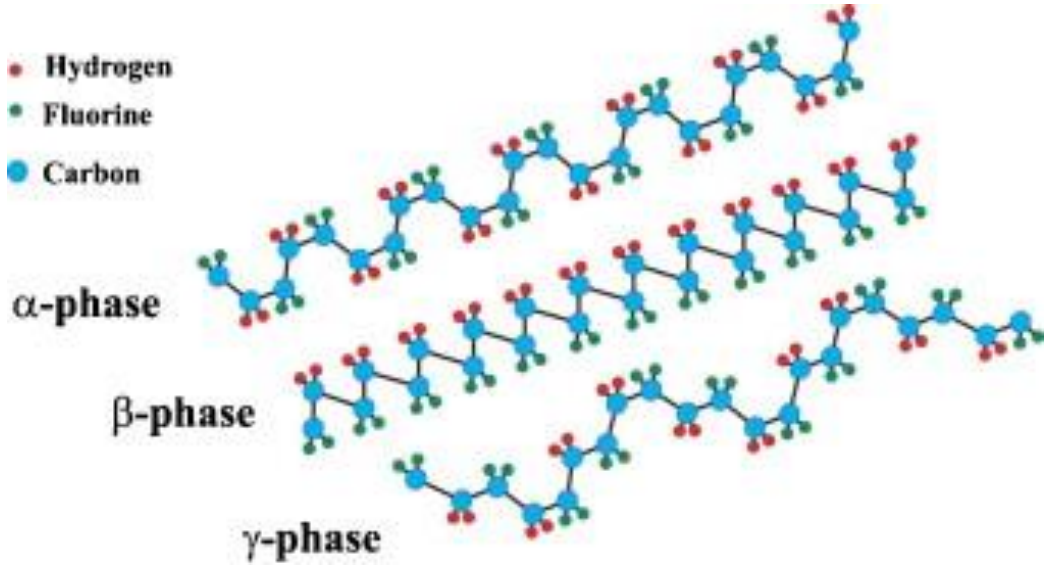

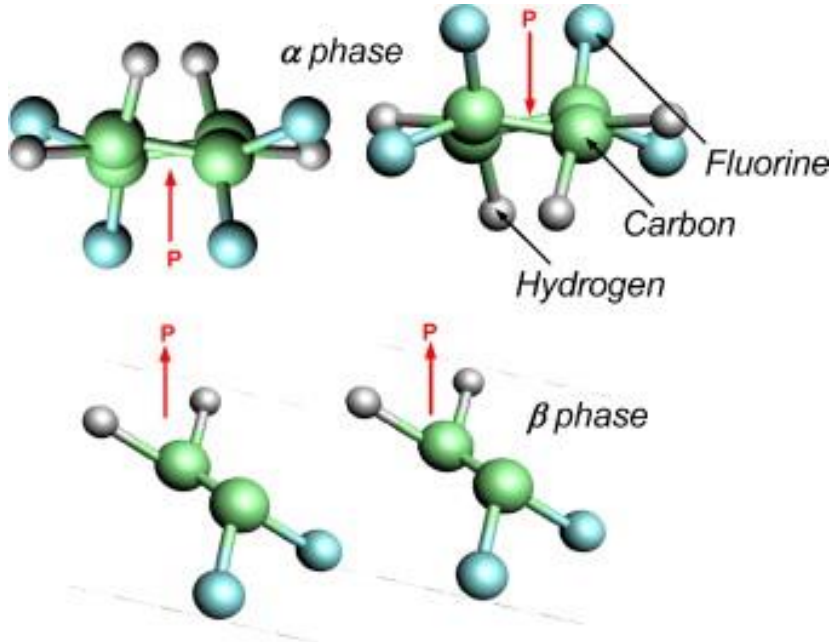

	Material	Piezoelectric constant (pico Coulombs/N)	Ref.
Polymers	Poly(L-lactide) (PLLA)	$d_{14} = -9.82$	[14,33]
	Poly(vinylidene fluoride) (PVDF)	$d_{33} = -32^{\S}$, $d_{31} = 6.7^{*}$	[34–37]
	Poly(vinylidene fluoride-trifluro ethylene) (PVDF-TrFE)	$d_{33} = -25.2$ to $-38^{\S}$	[38–40]
	Polyhydroxybutyrate (PHB)	$d_{14} = 1$ to 2	[12,41]
Ceramics	Hydroxyapatite (HA)	$d_{33} = 1.5$ to 2.4	[42]
	Barium titanate (BT)	$d_{33} = 191$	[14,43]
	Lithium sodium potassium niobate (LNKN)	$d_{33} = 98$	[44]
	Lithium niobate (LN)	$d_{33} = 23$	[45]
	Boron nitride nanotubes (BNNT)**	$d_{33} = 0.3$	[14,46]
	Potassium sodium niobate (KNN)	$d_{33} = 93$	[47]
Natural materials	Diphenylalanine (FF)**	$d_{33} = 18$, $d_{31} = 4$	[48]
	Collagen**	$d_{15} \sim 2$	[14,18,49]
	Bone	$d_{15} = 0.1$ to 0.7	[50,51]
	Silk**	$d_{14} = -1.5$	[52]
Composites	HA/BT	$d_{33} = 0.6$ to $2.8^{\pm}$	[30,53]
	LNKN/HA	$d_{33} = 2^{\pm}$	[54]

Courtesy: Progress in Polymer Science 39 (2014) 683–706; Surmenev et al, Nano Energy, 2019; Sensors and Actuators A: Physical Volume 177, April 2012, Pages 87-92

Piezoelectric polymers for biomedical applications

Most of the major functions in cells and organs of the human body are controlled by electrical signals. Piezoelectricity can be found in different parts of the human body.

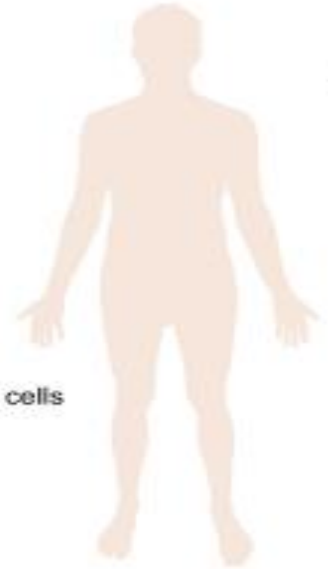

Electric

Corneal cells
Epidermal cells
Nervous system
Retinal cells
Vascular endothelial cells

Piezoelectric

Bone
Cartilage
DNA
Ligaments
Skin
Tendons

In vitro and *in vivo* studies of the piezoelectric polymers have been reported with greater effect than nonpiezoelectric materials. The MOST significant effect was observed in case of **nonbiodegradable** polymer – PVDF is strongest piezoelectric polymers

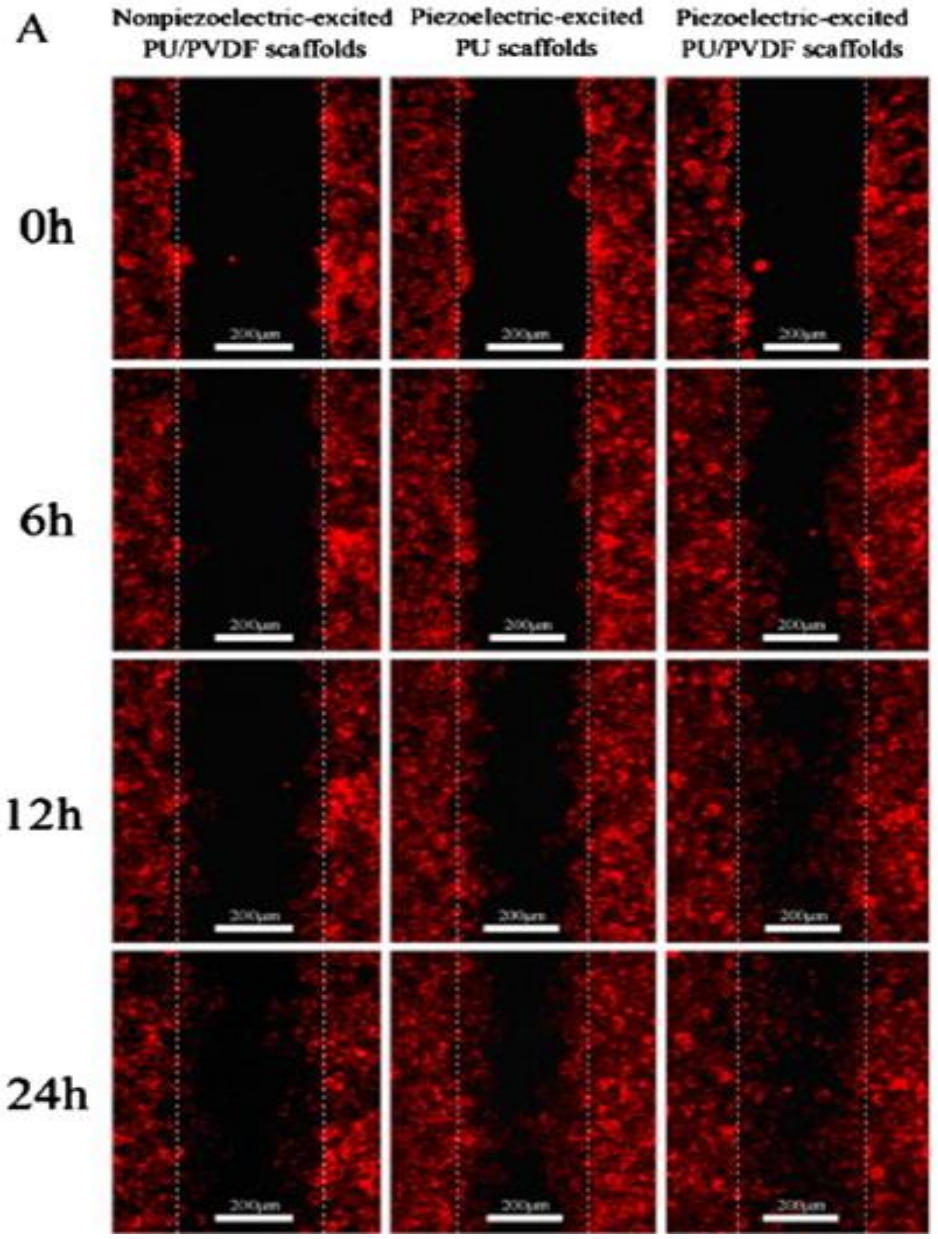

A.H. Rajabi et al. / Acta Biomaterialia 24 (2015) 12–23

Piezoelectric scaffold squeezes cells into action

The scaffold is made from the piezoelectric polymer poly(vinylidene fluoridetriflouroethylene) (PVDF-TrFE) using electrospinning in which an electric field is applied to the ejected polymer solution.

When the scaffold is deformed mechanically, electrical activity is generated without the need for any external power source or electrodes.

“Electrical stimulation has been shown to stimulate both cell growth and differentiation.”

In a bioreactor the as-spun piezoelectric PVDF-TrFE scaffolds promote the differentiation of stem cells into cartilage cells. The more strongly piezoelectric annealed scaffolds, by contrast, promote differentiation into bone cells.

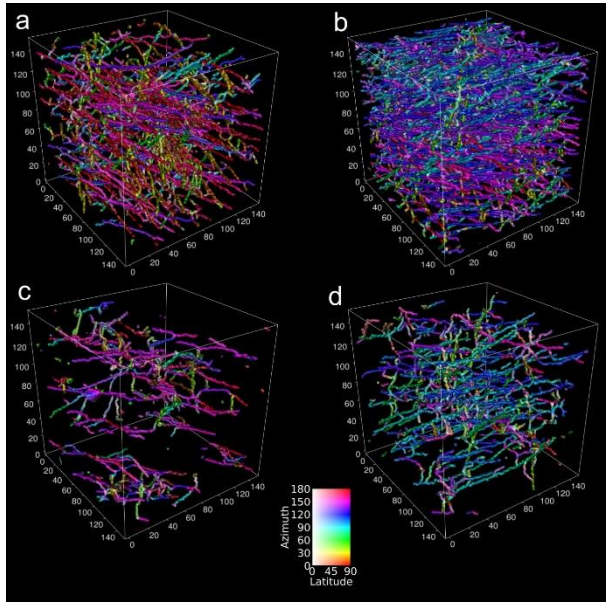

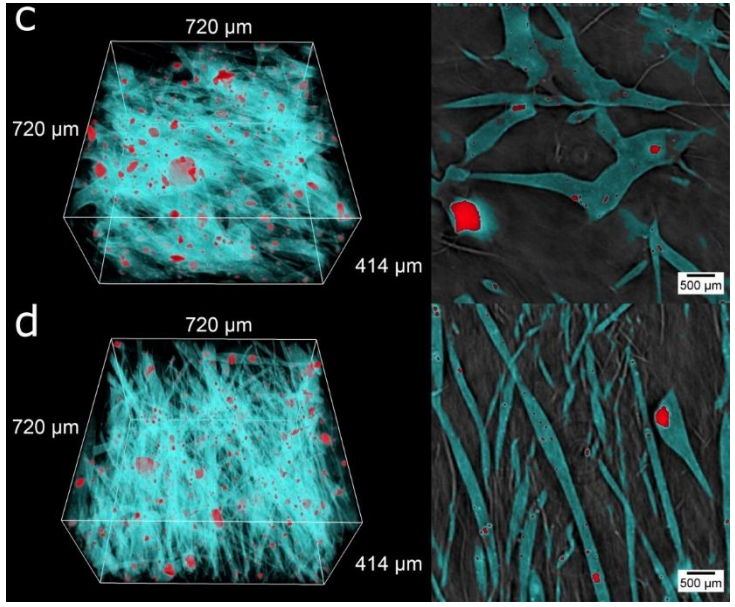

Microcomputed tomography of an electrospun scaffold

Gorozha, Surmenev et al, Scientific reports, 2018, Cordelia Sealy, Materials Today, 1369-7021/https://doi.org/10.1016/j.mattod.2018.01.022
By Treena Livingston Arinzeh of New Jersey Institute of Technology, who led the research with colleagues from the University of Washington and Shenzen Institutes of Advanced Technology in China.

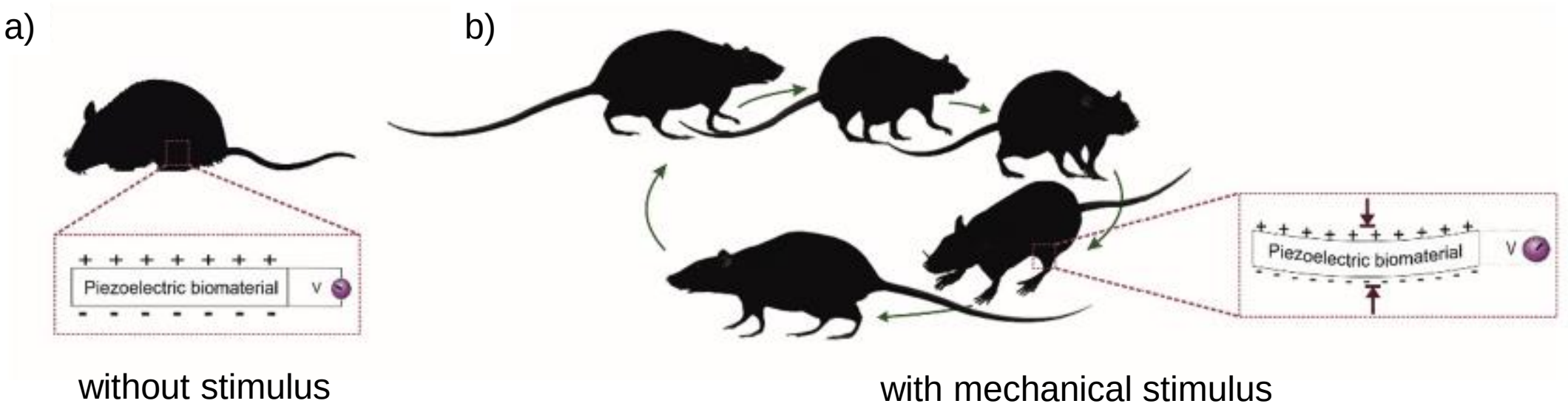

Schematic representation of the piezoelectric effect (with piezoelectric material implantation) (a) without and (b) with mechanical stimulus.

After 4 weeks, defect implanted with poled β-PVDF films demonstrated significantly more defect closure and bone remodeling, showing the large potential of piezoelectric biomaterials for bone repair.

Materials Letters, Volume 209, 15 December 2017, Pages 118-121

Piezoelectric materials for energy-harvesting applications

- e-skin, biosensors (e.g. self-powered glucose sensor),
- mechanosensors, gas sensors,
- piezo-catalysis, piezoelectric antibacterial effect,
- *in vivo* energy harvesters, tissue engineering applications

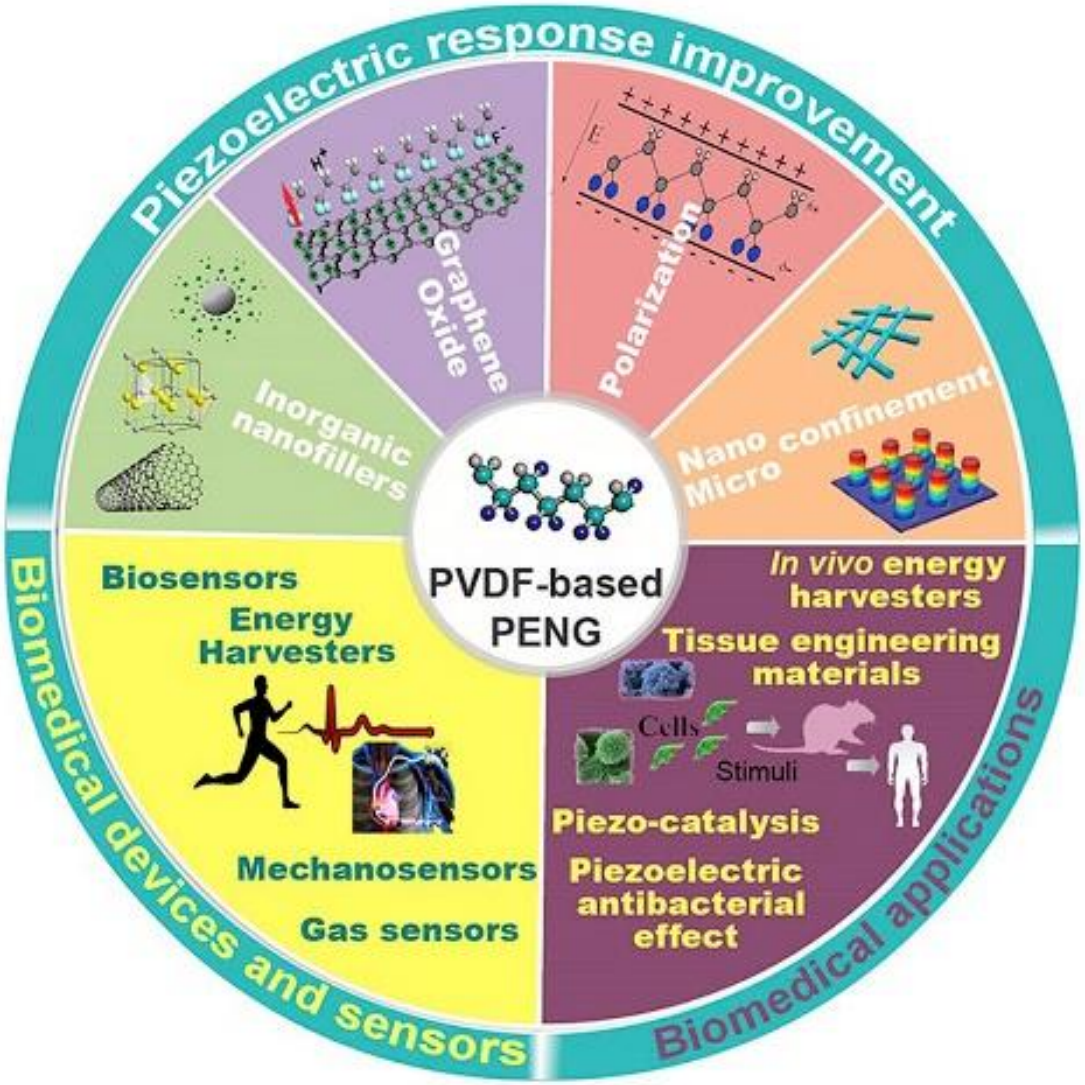

ELSEVIER

Nano Energy

Available online 30 April 2019

In Press, Accepted Manuscript

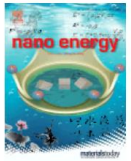

Review

Hybrid lead-free polymer-based scaffolds with improved piezoelectric response for biomedical energy-harvesting applications: A review

Roman A. Surmenev [a, b], Tetiana N. Orlova [a], Roman V. Chernozem [a], Anna A. Ivanova [a], Ausrine Bartasyte [c], Sanjay Mathur [b], Maria A. Surmeneva [a]

Show more

https://doi.org/10.1016/j.nanoen.2019.04.090

Contents lists available at ScienceDirect

Nano Energy

journal homepage: http://www.elsevier.com/locate/nanoen

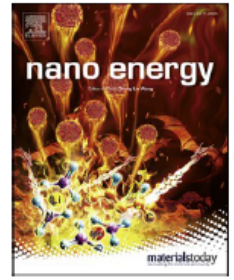

Review

A review on piezo- and pyroelectric responses of flexible nano- and micropatterned polymer surfaces for biomedical sensing and energy harvesting applications

Roman A. Surmenev *, Roman V. Chernozem, Igor O. Pariy, Maria A. Surmeneva

Physical Materials Science and Composite Materials Centre, Research School of Chemistry & Applied Biomedical Sciences, National Research Tomsk Polytechnic University, Lenin Avenue 30, 634050 Tomsk, Russia

ARTICLE INFO

Keywords:
PVDF
PVDF-TrFE
Nanoconfinement
Piezoresponse
Energy harvesting
Sensors
Piezoelectric nanogenerators

ABSTRACT

This review summarises the most recent advances in the application of anodic aluminium oxide (AAO) membranes as templates to prepare poly(vinylidenefluoride)-(PVDF) or poly(vinylidenefluoride-co-trifluoroethylene)-based (PVDF-TrFE) piezoelectric generators, which are typically utilised in biomedical sensing and energy harvesting applications. The significant variation in the electroactive phase content in PVDF or PVDF-TrFE caused by the enhanced polarisation of AAO membranes due to nanoconfinement effect is explored. The literat[illegible]erformances of various devices are significantly im[illegible]t films with the same material composition. Thus, nano- and microstructuring of the surface of biocompatible piezopolymers is promising for their applications in

In vivo energy harvesting

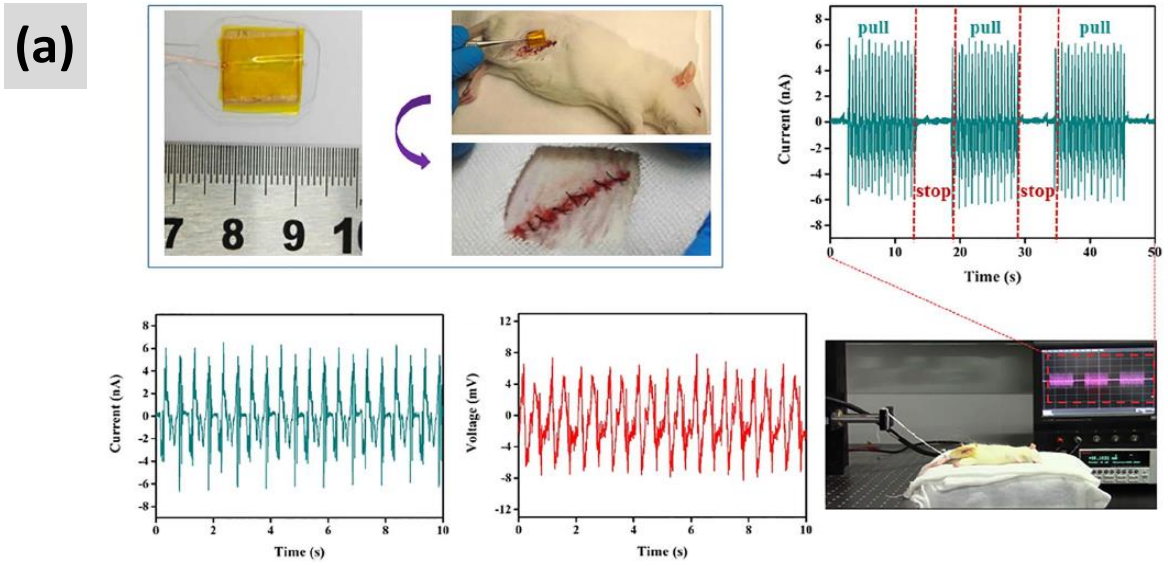

(*a*) *In vivo* наногенератор на основе нановолкнистых электроформованных PVDF-TrFE скэффолдов (*Wang A., Liu Z., Hu M., Wang C., Zhang X., Shi B., Fan Y., Cui Y., Li Z., Ren K.* Piezoelectric nanofibrous scaffolds as in vivo energy harvesters for modifying fibroblast alignment and proliferation in wound healing // Nano Energy. 2018. Vol. 43. P. 63–71.) и (*b*) PVDF пленка, упакованная в PDMS/парилен-С. На фотографиях (i)–(v) показан типичный хирургический процесс имплантации наногенератора и заживление раны в области имплантации через день и шесть месяцев после проведения операции (*Li J., Kang L., Yu Y., Long Y., Jeffery J.J., Cai W., Wang X.* Study of long-term biocompatibility and bio-safety of implantable nanogenerators // Nano Energy. 2018. Vol. 51. P. 728–735.)

An autonomous glucose sensor

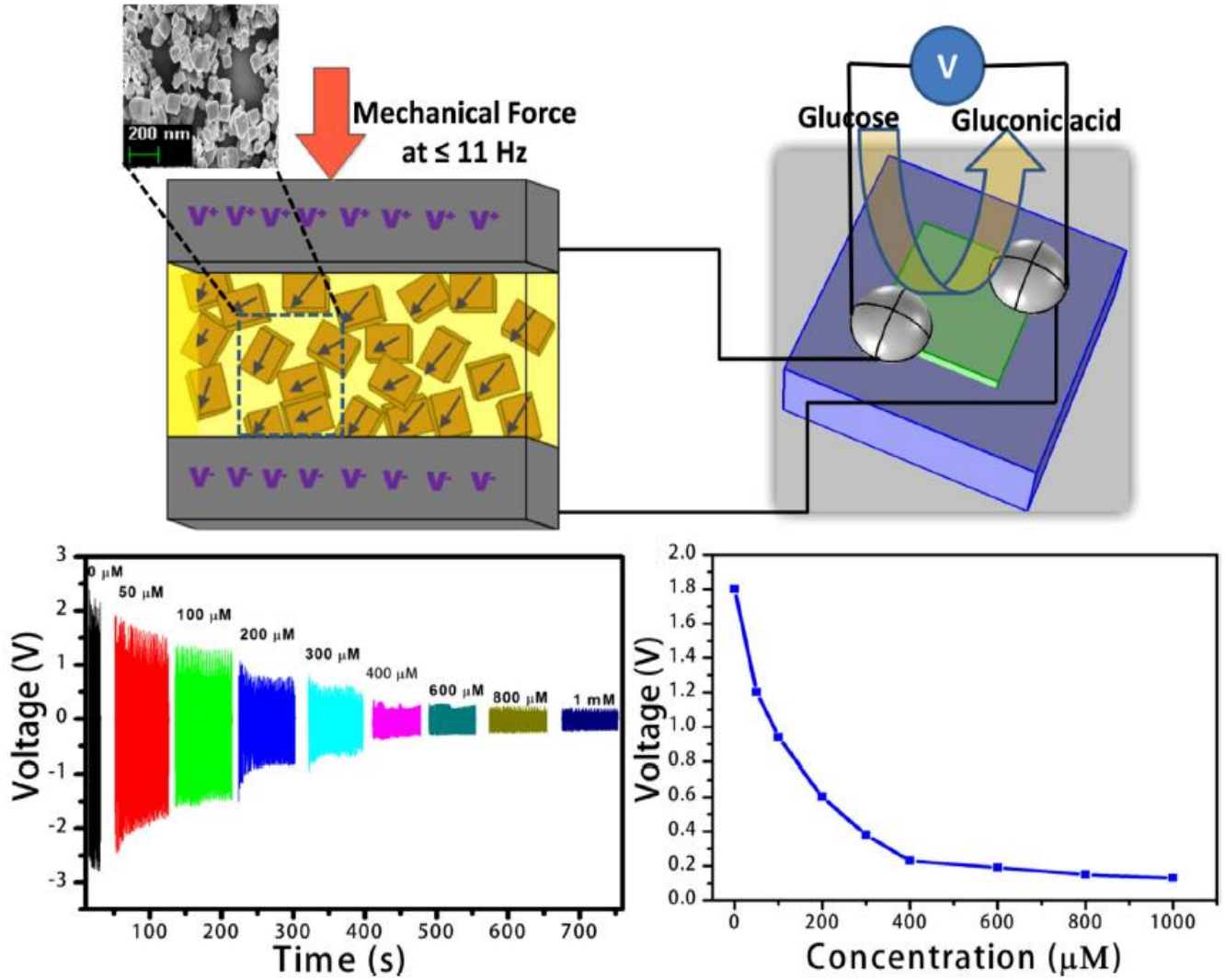

Future Outlook

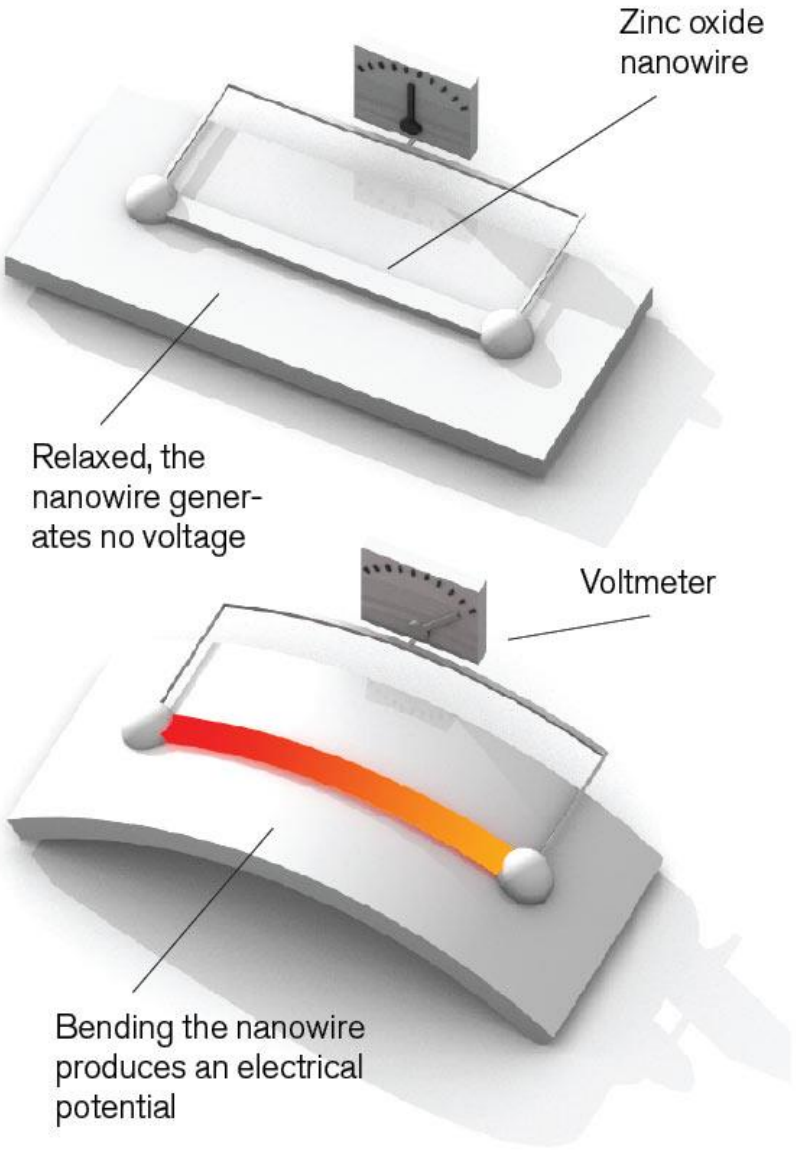

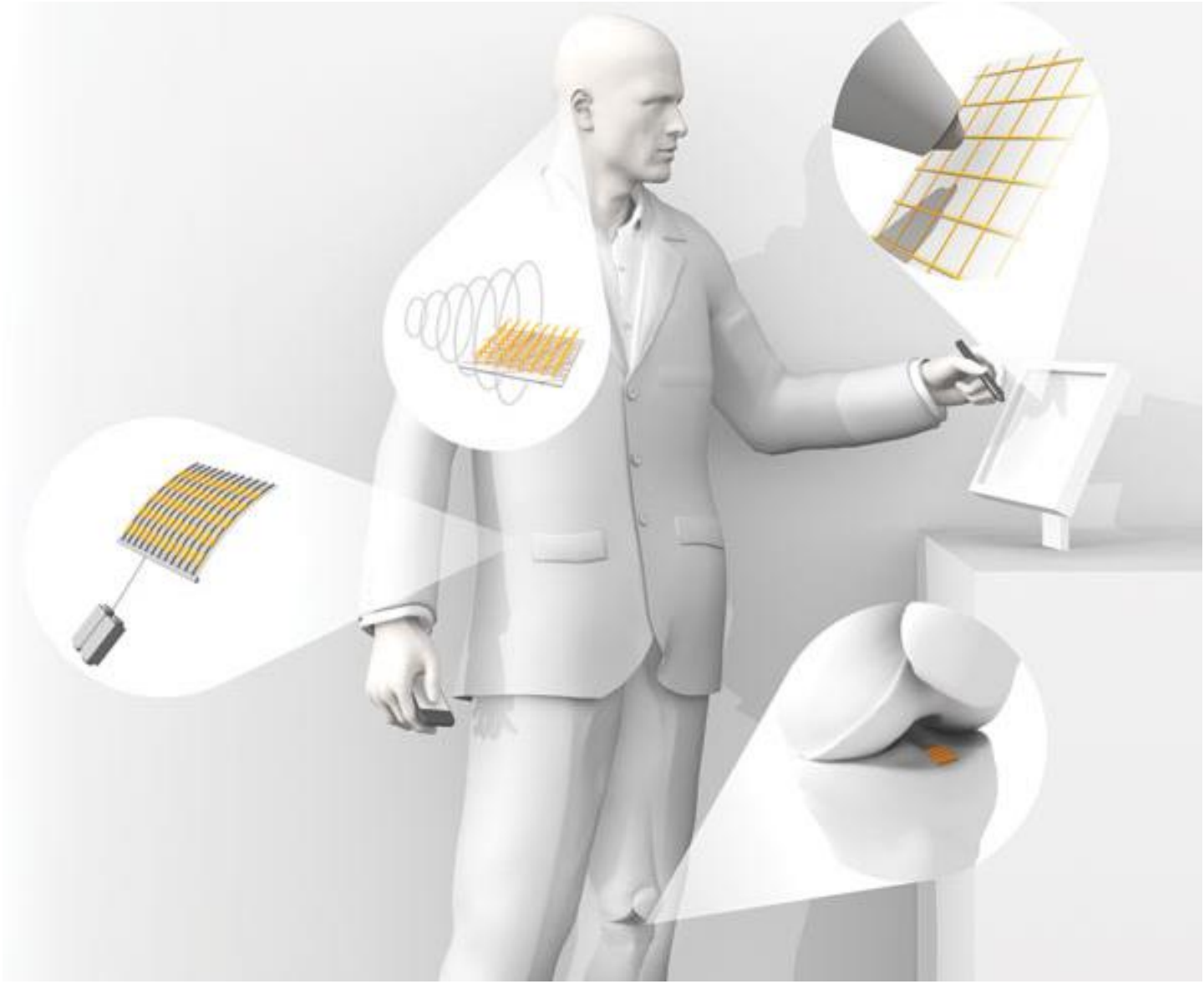

Courtesy: ARSLAN MAJID, University of Utah, USA

Piezoelectrically enhanced photocatalysis

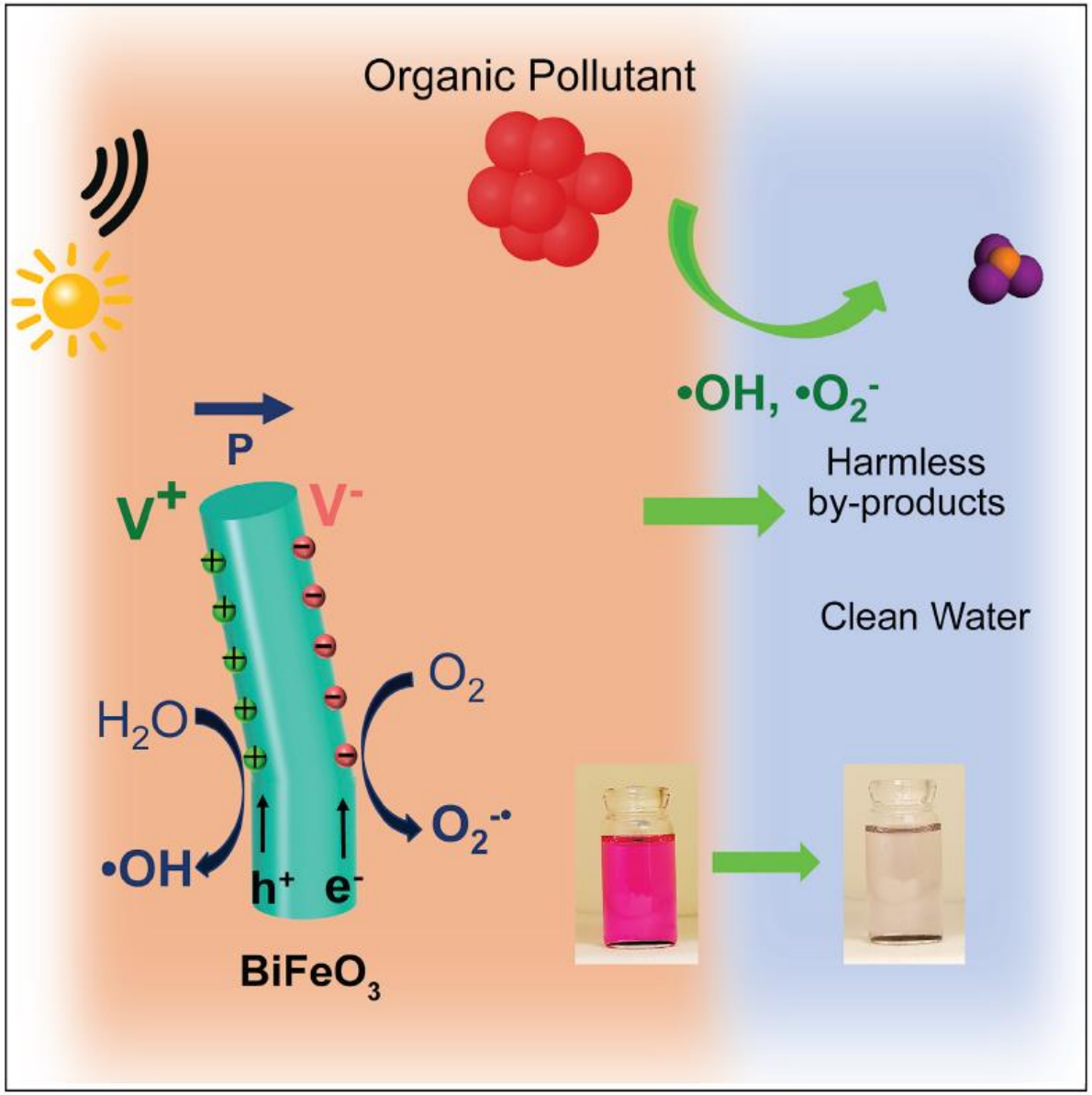

Aim: water cleaning or pollution removal, e.g. rhodamine B (RhB) dye, methyl orange dye

Objective: photocatalytic activity under UV-visible light

Materials: PVDF-TrFE with $BiFeO_3$ or $BaTiO_3$

Effect: Piezocatalytic degradation

$$BiFeO_3 + h\upsilon \text{ or US} \rightarrow BiFeO_3\,(e^- + h^+)$$

$$e^- + O_2 \rightarrow O_2^{-\cdot}$$

$$h^+ + H_2O \rightarrow \cdot OH$$

$$h^+ + RhB \rightarrow \text{degradation products}$$

$$\cdot OH + RhB \rightarrow \text{degradation products}$$

iScience 4, 2018, 236-246

Applications of piezoelectric materials

- **Sensors**
- Microphones, pick-ups
- Pressure sensor
- Force sensor
- Strain gauge

- **Actuators**
- Loudspeaker
- Piezoelectric motors
- Nanopositioning in AFM, STM
- Acusto-optic modulators
- valves

- **High-voltage and power source**
- Cigarette lighter
- Energy harvesting
- AC voltage multiplier

- **Frequency standard**

Acro-scale Piezoelectric applications

The “quartz resonator” for use as a timing standard

- - The frequency of the oscillator is determined by the cut and shape of the quartz crystal.
- -Miniature encapsulated tuning forks which vibrate **32,768 times per second**

Piezoelectric lighter

The image is the public domain

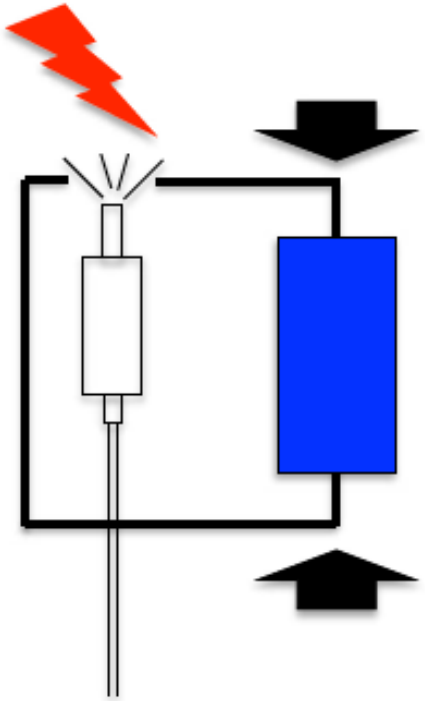

Mechanical shock is converted to electricity

Breakdown voltage in air?

- A small, spring-powered hammer rise off the surface of the piezo crystal strikes the crystal as the gas is turned on. The impact creates a large voltage across the crystal, and therefore a spark between the wires, which ignites the gas.

Atomic Force Microscope

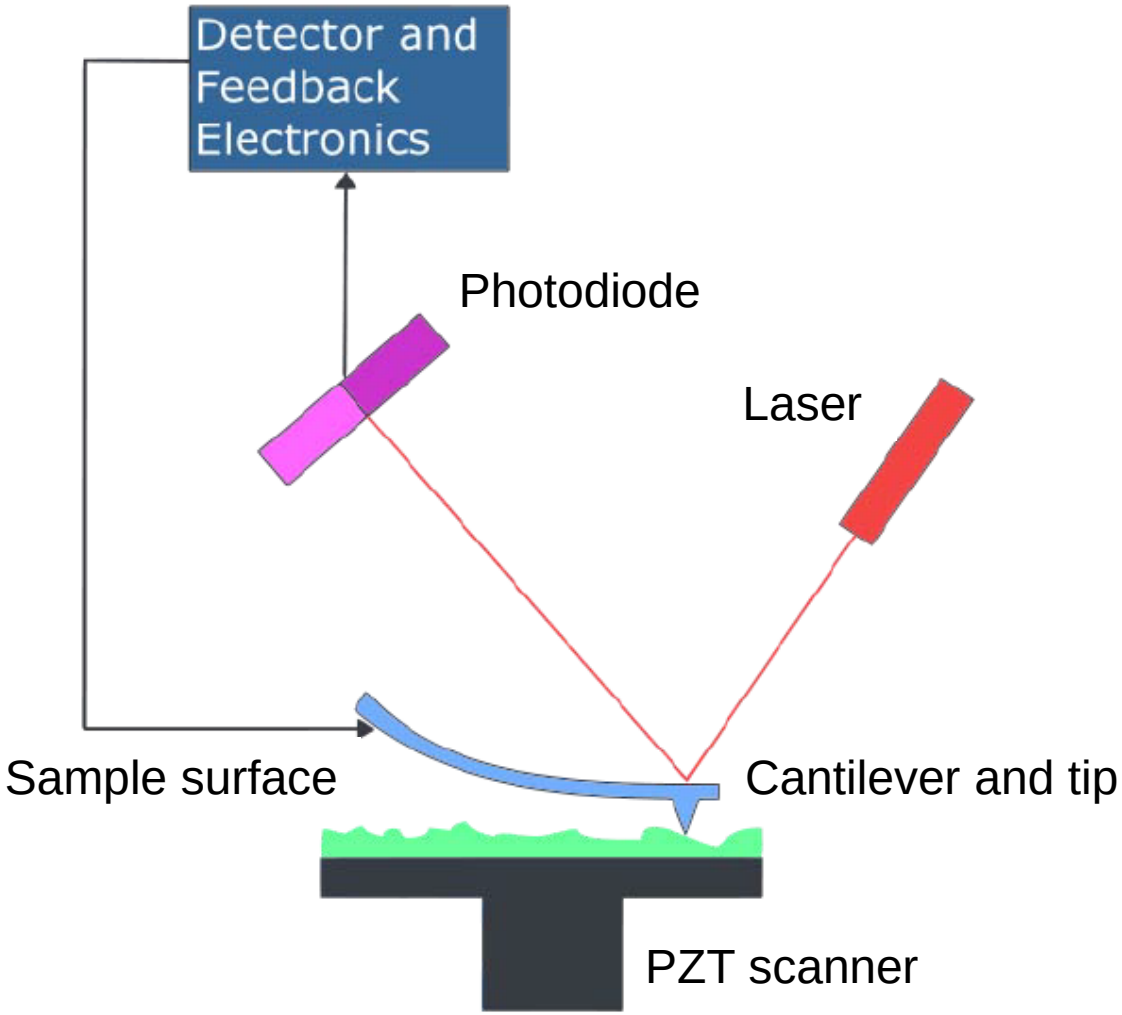

Applications of pressure sensors

- Touch screen devices
- Automotive industry
- Biomedical
- Aviation
- Marine industry (SONAR - SOund NAvigation Ranging)

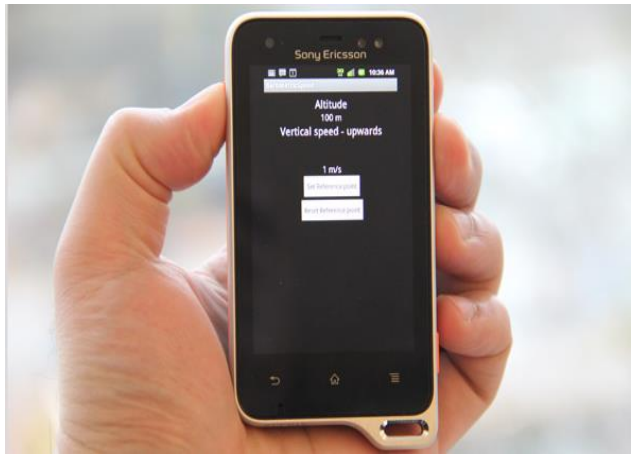

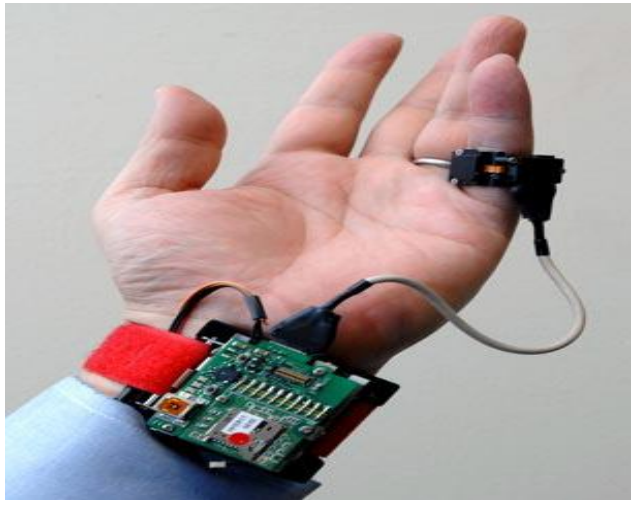

Consumer Electronics Applications

- Quartz crystals resonators as frequency stabilizers for oscillators in all computers.
- Phonograph pick-ups
- **Accelerometers**: In a piezoelectric accelerometer a mass is attached to a spring that is attached to a piezoelectric crystal. When subjected to vibration the mass compresses and stretches the piezo electric crystal. (iPhone)

Motor Applications

- Piezoelectric elements can be used in laser mirror alignment, where their ability to move a large mass (the mirror mount) over microscopic distances is exploited. By electronically vibrating the mirror it gives the light reflected off it a Doppler shift to fine tune the laser's frequency.
- The piezo motor is viewed as a high-precision replacement for the stepper motor.
- Traveling-wave motors used for auto-focus in cameras.

Magnetoelectric materials and applications

Multiferroics

Multiferroics are defined as materials that exhibit more than one of the primary ferroic order parameters in the same phase « formation of switchable domains:

Ferromagnetism **Ferroelectricity**
Ferroelasticity

spontaneous spontaneous spontaneous

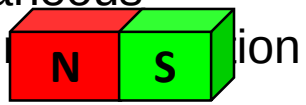

ion

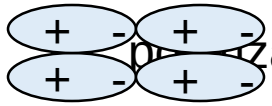

zation

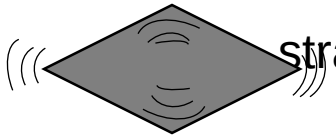

strain

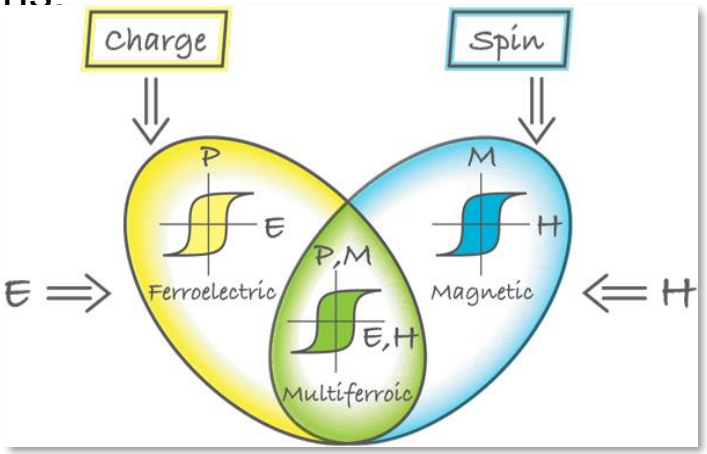

Ferroelectric ***Ferroelastic***

Piezoelectric and electrostrictive coupling

Ferromagnetic ***Ferroelastic***

Piezomagnetic and magnetomechanical coupling

Ferromagnetic ***Ferroelectric***

Magnetostrictive and piezoelectric coupling

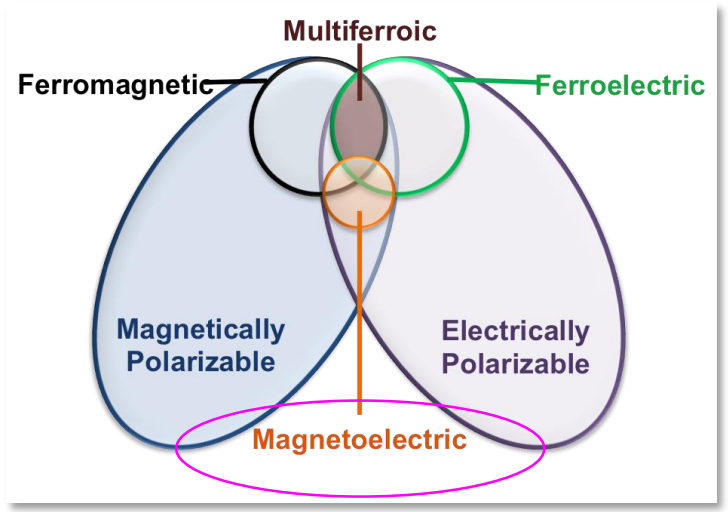

Magnetoelectric effect

The **magnetoelectric effect** (ME) is the phenomenon of inducing magnetic (electric) polarization by applying an external electric (magnetic) field. The effects can be linear or/and non-linear with respect to the external fields. Only a few single-phase materials have significant ME effect at room temperature.

1) $P_i = \Sigma\alpha_{ij} H_j + \Sigma\beta_{ijk} H_j H_k + \ldots..$

2) $M_i = \Sigma\alpha_{ij} E_j + \Sigma\beta_{ijk} E_j E_k + \ldots\ldots\ldots$

Two types

- **1) Direct ME effect**
- **2) Converse ME effect**

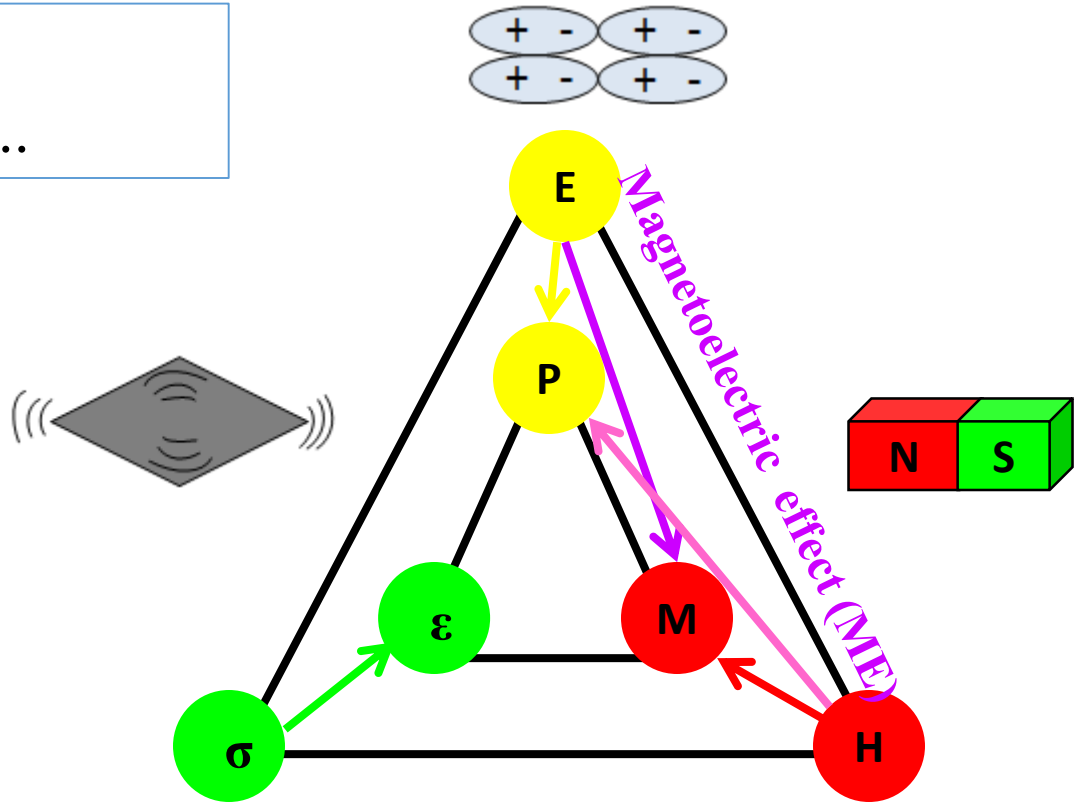

History of the topic

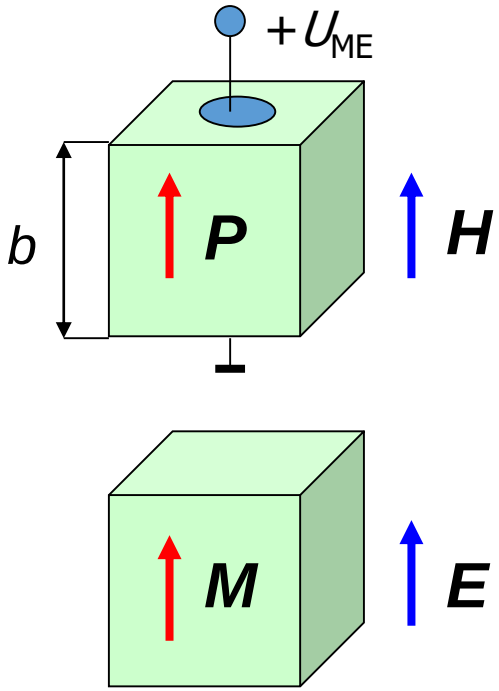

The **magnetoelectric (ME) effect** is defined as the dielectric polarization of a material in an applied magnetic field ***H*** (**direct effect**) or an induced magnetization in an external electrical field ***E*** (**inverse effect**)

$P = \alpha_{ik} H$, where α_{ik} is the magnetoelectric tensor.

The ME effect exists in materials which have simultaneous presence of long-range ordering of magnetic moments and electric dipoles

The ME effect was first pointed out by **P. Curie** in 1894 and explained by **L. Landau and E. Lifshitz** in 1960

D. Astrov observed **inverse ME** interaction in a Cr_2O_3 single crystal in 1960

V. Folen and G. Rado observed **direct ME** interaction in Cr_2O_3 single crystal in 1961

The ME interaction is weak in single crystals and observed at low temperatures.
The effect can be **2 - 4 orders in magnitude** stronger in **composite structures** !!

Magnetoelectric effect in composites

1. Direct ME effect

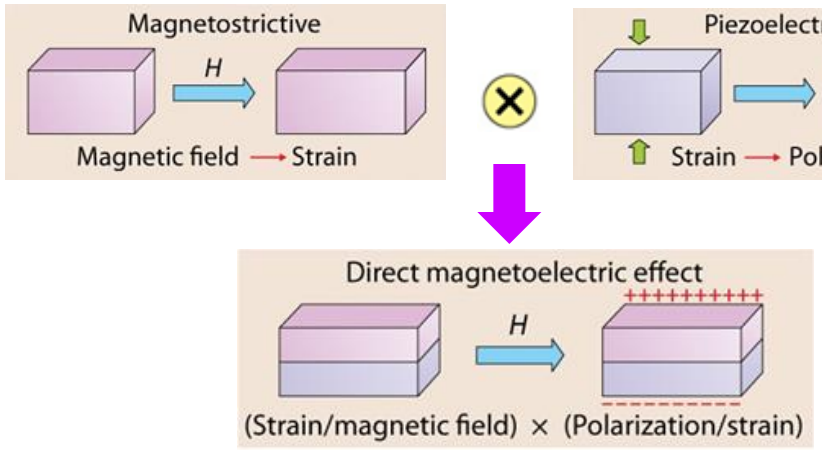

- Mechanical deformation of the magnetostrictive phase

2. Converse ME effect

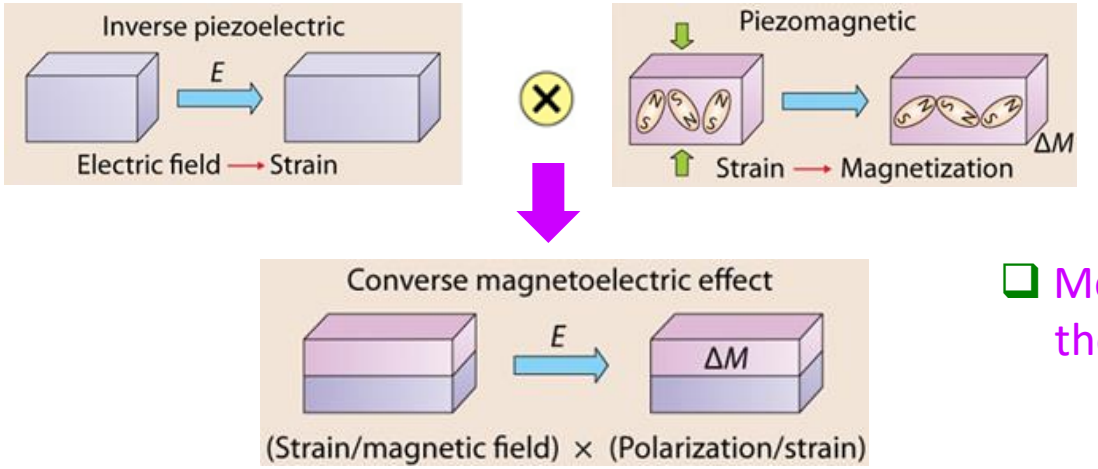

- Mechanical deformation of the piezoelectric phase

ME effect = piezoeffect+magnetostriction

$$\mathrm{ME_H}\ effect = \frac{Electrical}{Mechanical} \times \frac{Mechanical}{Magnetic};$$

Piezoelectricity ***Magnetostriction***

$$\alpha_{ij} = (\partial P_i/\partial H_j) = k_c(\partial P_i/\partial T_k)\,(\partial T_k/\partial S_l)(\partial S_l/\partial H_j) = k_c d_{ik} s_{kl}^{-1} q_{jl};$$

✓ Direct ME open-circuit (D_3=0) voltage coefficient (α_{Eij}) ca. proportional to ratio between d and ε:

$$\alpha_{Eij} = \partial E_i/\partial H_j = \alpha_{ij}/\varepsilon_{ij}, \qquad (V/(cm\cdot Oe))$$

+resonance+charge effects+exchange bias+spin effects+…

Magnetic field and current sensors

Традиционная энцефалограмма

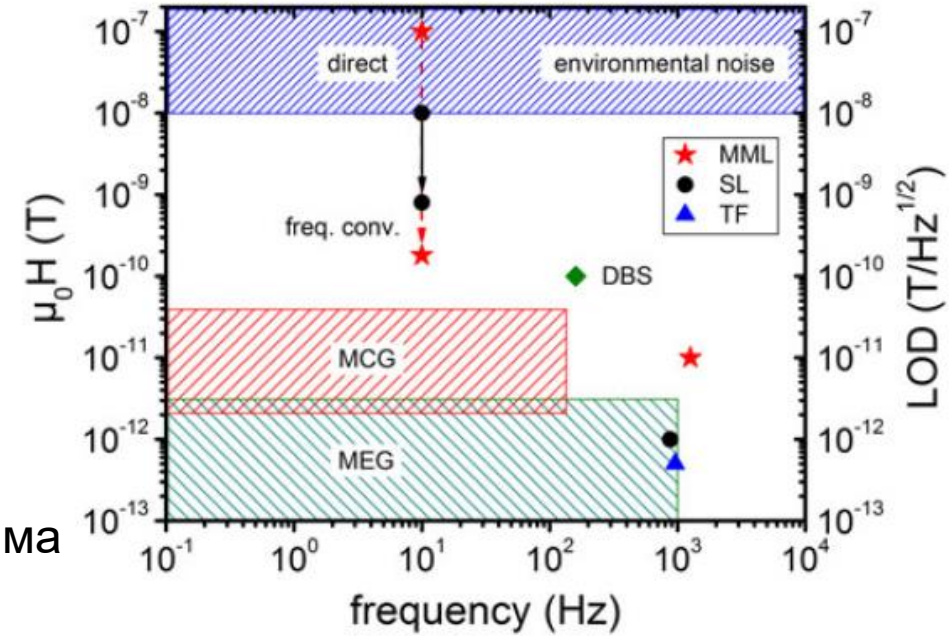

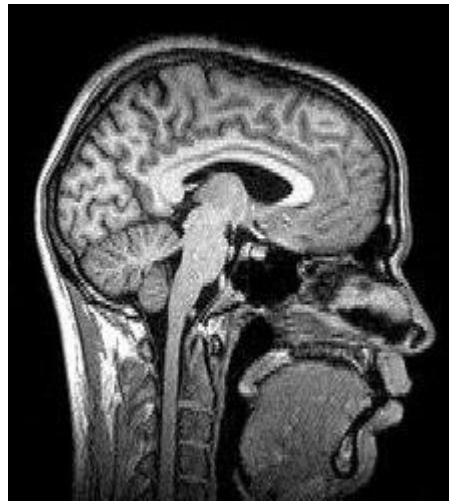

МР томограмма

Магнитная энцефалограмма (SQUID)

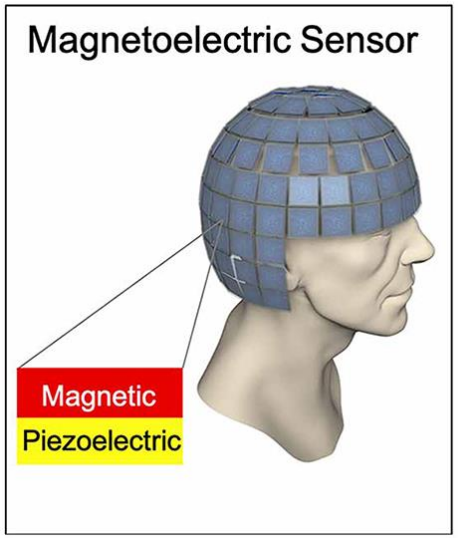

Магнитная энцефалограмма (МЭ эффект)

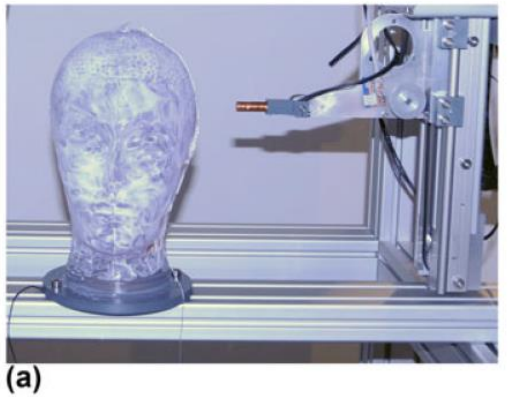

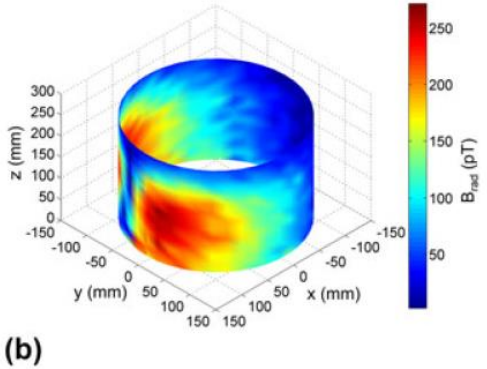

Röbisch et al., J. Materials Res. 32 , 1009 (201

Biomedical applications of magnetoelectric (ME) materials

- ME of a various form and shape: nanoparticles, nanowires, etc.
- Targeted drug delivery (in particular for cancer treatment)
- Treatment of Alzheimer's and Parkinson's diseases
- Magnetoelectric materials for miniature, wireless neural stimulation at therapeutic frequencies (up to 200 Hz)
- Skeletal muscle tissue regeneration, bone tissue regeneration etc
- Wireless power supply to:
- neurostumulators (spinal cord stimulation systems) for pain relief,
- magnetoelectric composites (for wirelessly powered brain implantable devices)
- …
- Magnetoelectrically driven catalytic degradation of organics etc.

Concept of ME nanorobots

Micro/nanorobots fabrication	Magnetic component	
• Photolithography • Two-photon lithography/ Direct laser writing / 3D laser lithography • Glancing angle deposition • Template-assisted electrodeposition • Biotemplate method	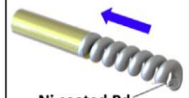	▪ Magnetic films • e-beam evaporation • Physical vapor deposition/ sputter deposition • Dip-coating
		▪ Magnetic segments • Electrodeposition • Oblique angle deposition
		▪ Magnetic particles • Dip-coating • Emulsion method

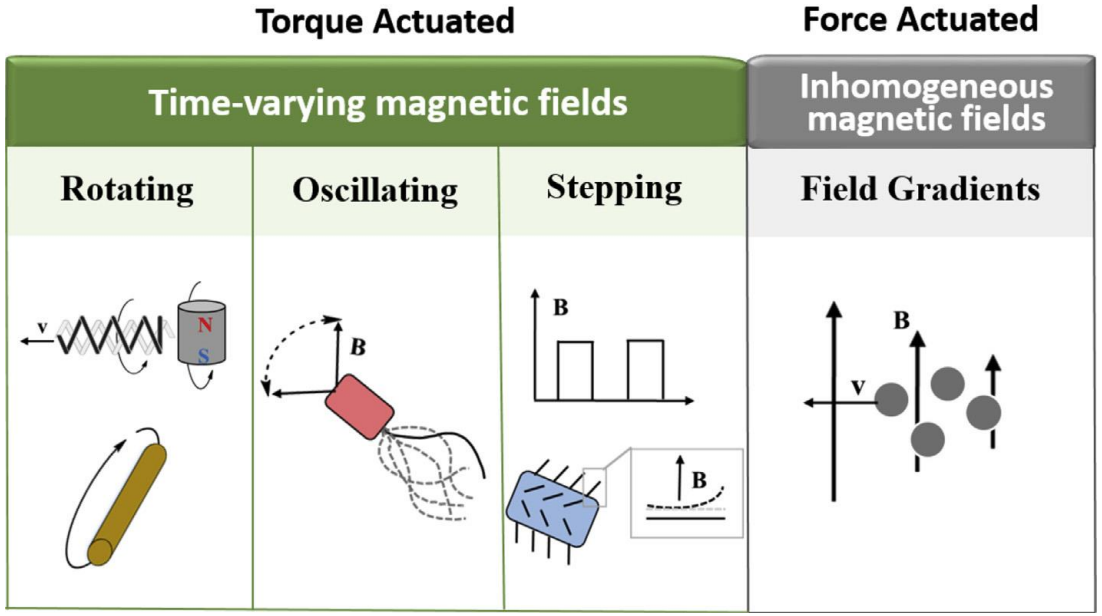

Usually core-shell nanoparticles - $CoFe_2O_4$ (core) and either $BaTiO_3$ or PVDF or PVDF-TrFE or etc (shell)

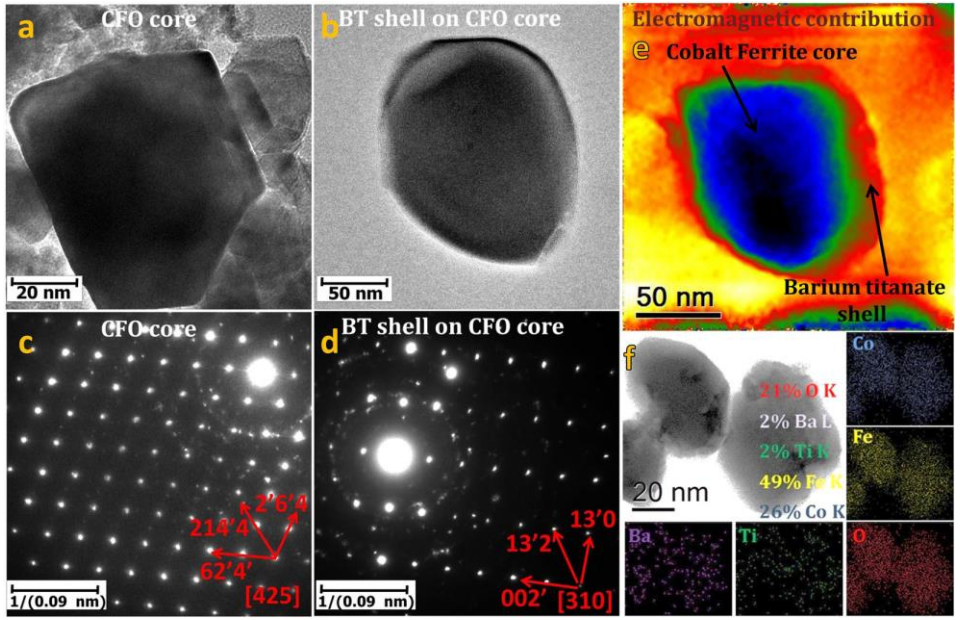

Materials Today Bio 8 (2020) 100085
Scientific reports | (2018) 8:1755

ME nanorobots

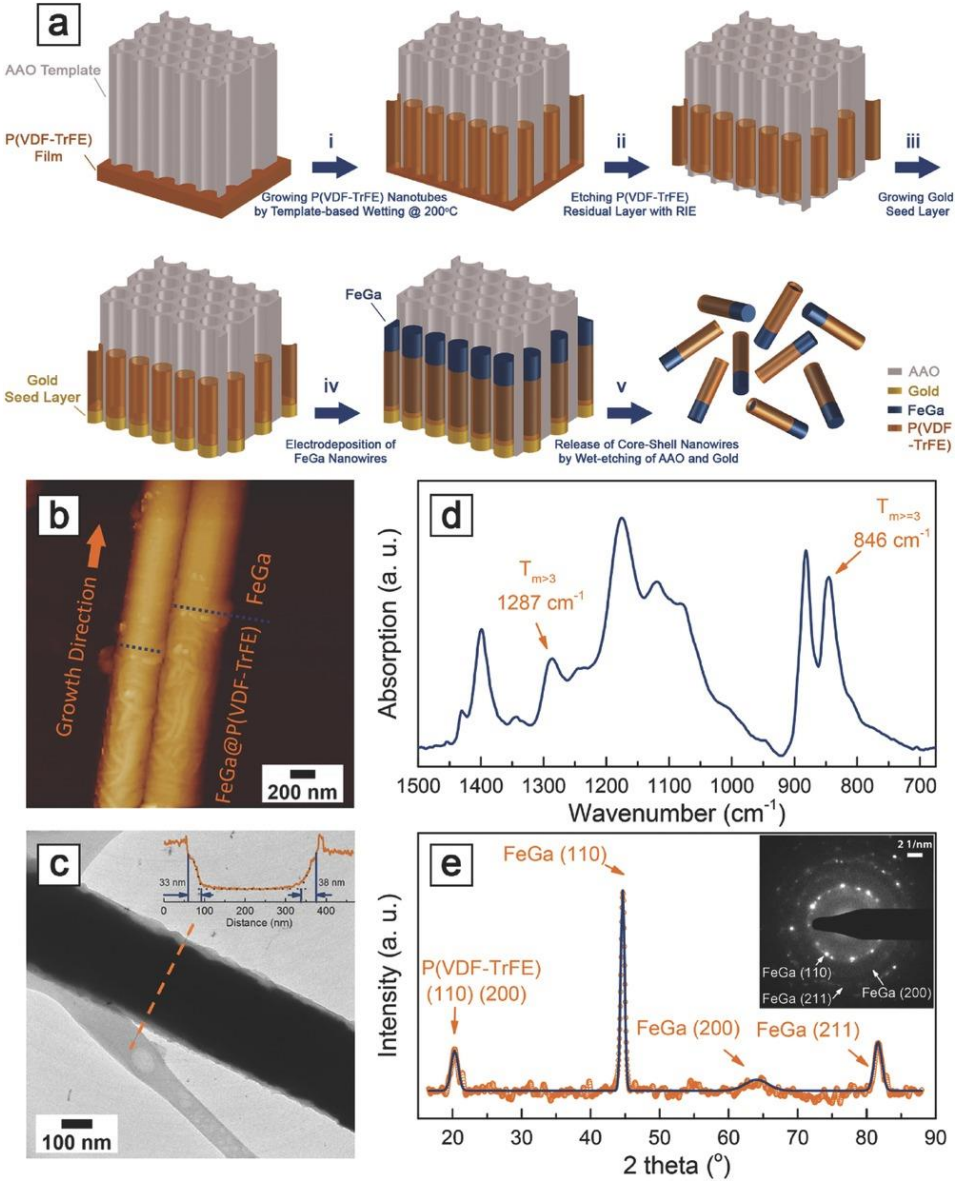

a) Fabrication scheme of FeGa@P(VDF-TrFE) core–shell nanowires. b) AFM image of two nanowires with FeGa grown out of P(VDF-TrFE) nanotubes. The arrow indicates the growth direction of FeGa. c) TEM image of a core–shell nanowire. The inset shows the cross-sectional grayscale profile along the dashed line. d) Infrared spectrum of P(VDF-TrFE) nanotubes. e) XRD pattern showing crystalline structure of FeGa@P(VDF-TrFE) core–shell nanowires. The inset shows the SAED pattern of a single nanowire.

Chen et al. Advanced Materials. DOI: 10.1002/adma.201605458

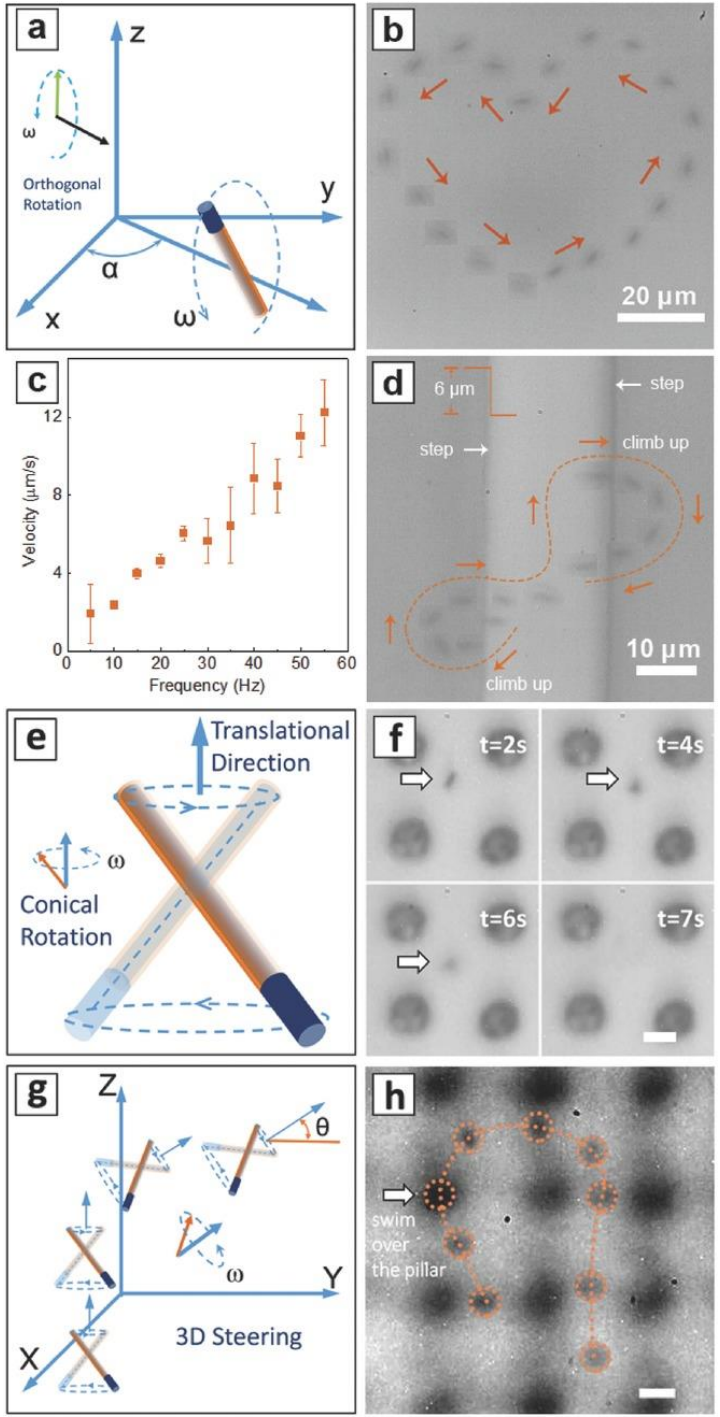

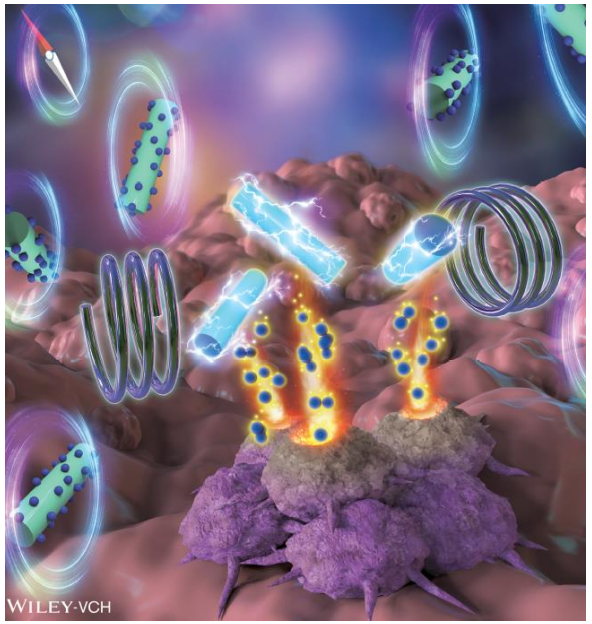

Schematic illustration of the nanowire rotating vertically with respect to the *x*–*y* plane. b) The nanowire is manipulated to follow the shape of a heart. c) Average translational velocity with respect to the magnetic field frequency. d) Demonstration of nanowire climbing up a step of 6 μm high. e) Schematic illustration of the motion of a core–shell nanowire in a conical rotating magnetic field. f) A core–shell nanowire moving away from the surface under the manipulation of a conical rotating magnetic field. g) Schematic illustration of steering the nanowire by changing the translational motion direction. h) The nanowire is steered to swim following a U-shaped trajectory. Scale bars in(f) and (h) represent 5 μm.

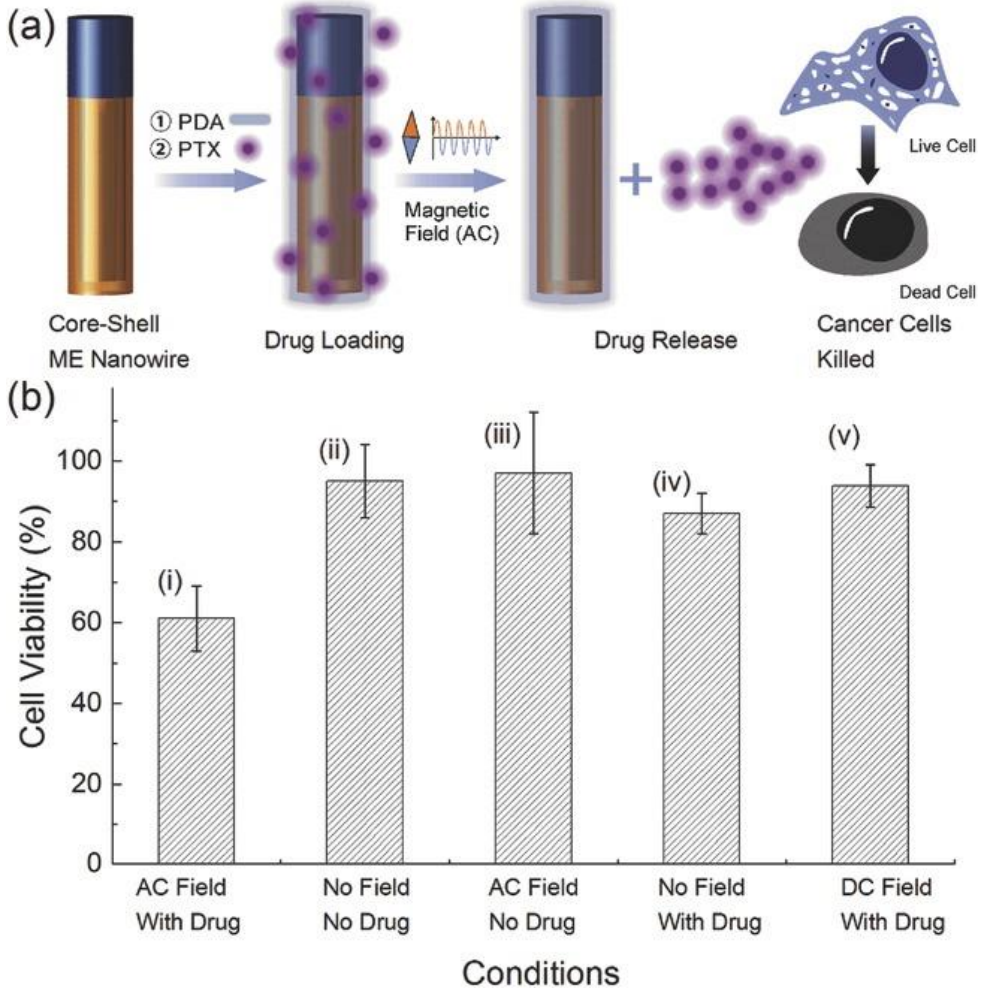

a) Scheme showing on-demand drug delivery experiment. The anticancer drug is loaded onto a PDA treated FeGa@P(VDF-TrFE) core–shell nanowire and then released by applying an alternating magnetic field. PDA: polydopamine. PTX: paclitaxel. b) The efficacy of AC field triggered on demand drug delivery experiment in comparison to several control experiments.

2021_Сурменев_апрель ПРФН_Магнитоэлектрические материалы_Surface walking.wmv

2021_Сурменев_апрель ПРФН_Магнитоэлектрические материалы_Climbing the wall.wmv

Chen et al. Advanced Materials. DOI: 10.1002/adma.201605458

Illustration of the underlying physics of the a.c.-field-triggered release

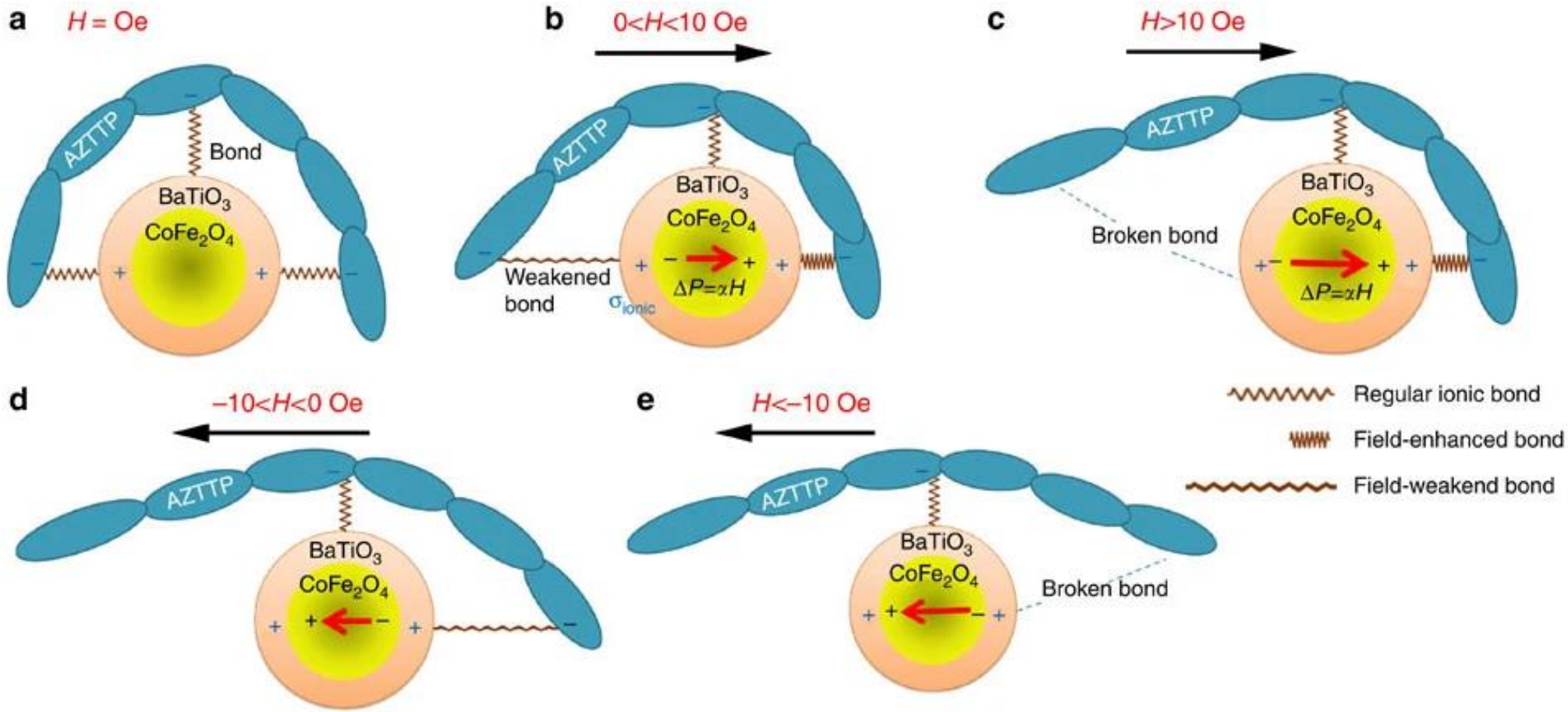

A simplified (one directional) illustration of the concept of on-demand drug (**Nucleotide reverse transcriptase inhibitor 3′-azido-3′-deoxythymidine-5′-triphosphate, AZTTP**) release by MENs stimulated by a uniform a.c. magnetic field in X direction. (**a**) At zero field, only the ionic charge is present in the MEN shell. (**b**) An additional dipole moment (proportional to the magnetic field) breaks the original symmetry of the charge distribution in the shell. (**c**) As the field is increased above the threshold value ($\sigma_{ionic} \sim \sigma_{ME}$), the bond on one side is broken. (**d**,**e**) The field is reversed to break the bond on the opposite side of the nanoparticle. The red arrows show the electric dipole due to the ME effect. In practice, owing to the random configurations of nanoformulations with respect to the field, the effect is present along every central bond orientation. 30 nm **$CoFe_2O_4$@$BaTiO_3$**

Nature Communications **volume 4**, Article number: 1707 (20

Magnetoelectric nanoparticles help the brain

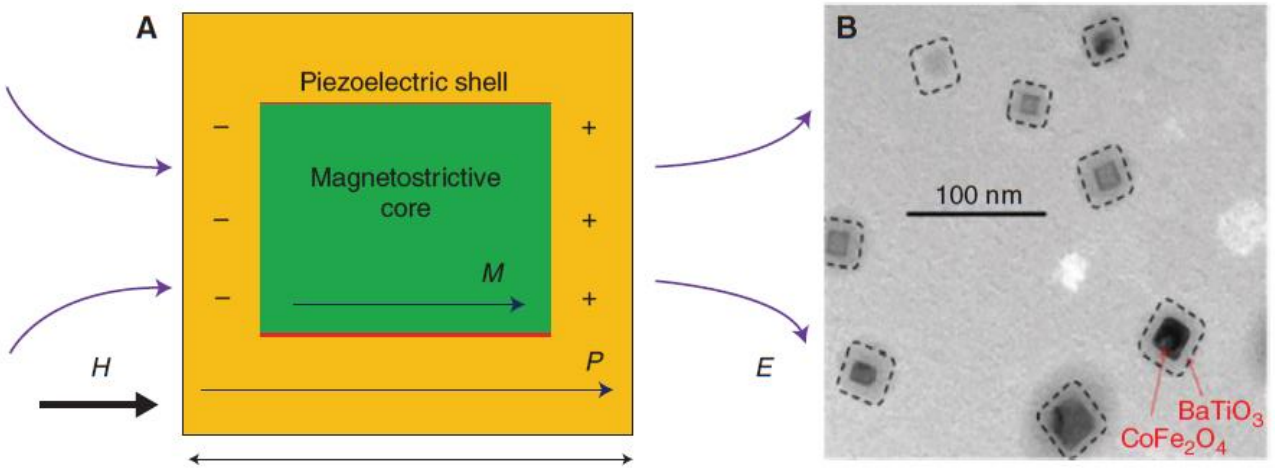

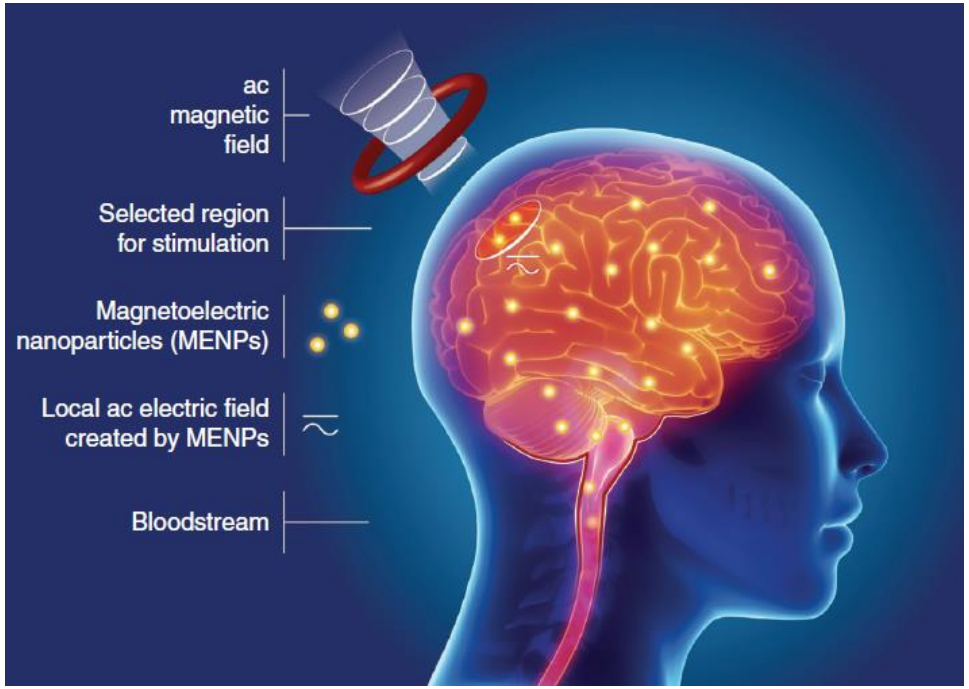

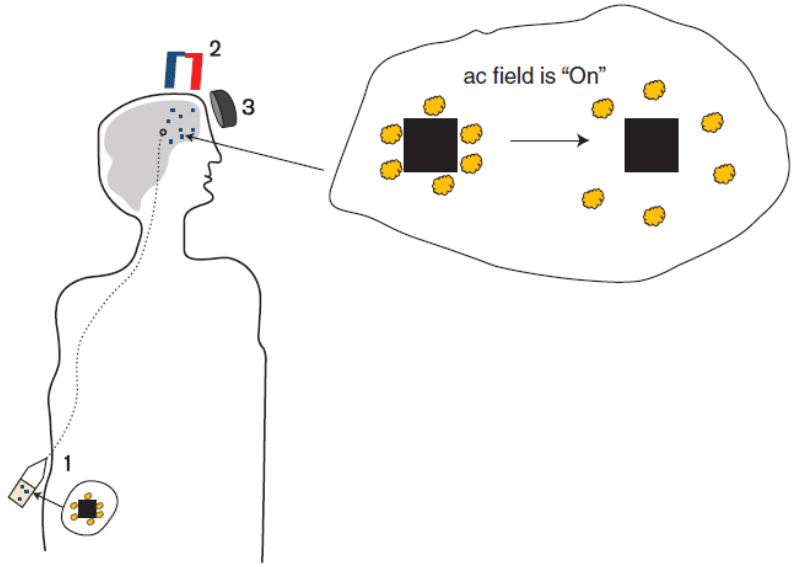

Khizroev, Cold Spring Harb Perspect Med. 9, a034207 (2

Bone regeneration using piezoelectric nanobiomaterials

Figure. a) Illustration of rapid osseointegration between electropositive implant and electronegative bone interaction. b) Histological evidence for pronounced osseointegration with BFO^{+} coated STO implants compared to uncoated or BiFeO3 (BFO^{-}) coated SrTiO3 (STO) implants (yellow arrows: bone-material interfaces; NB: nascent bone, FT: fibrous tissue). c) Schematic representation of mechanical strain induced electric charge generation on piezoelectric material surface triggering cell signaling pathways; d) Alkaline phosphatase activity after 15 d of static and dynamic culture of hASCs on different PVDF films using regular and osteogenic medium (*$p \leq 0.005$). e) Effects of US stimulation to cultured SaOS-2 cells on P(VDF-TrFE) and P(VDF-TrFE)/BNNT films using differentiation medium (Bright-field microscopy after Alizarin Red staining).

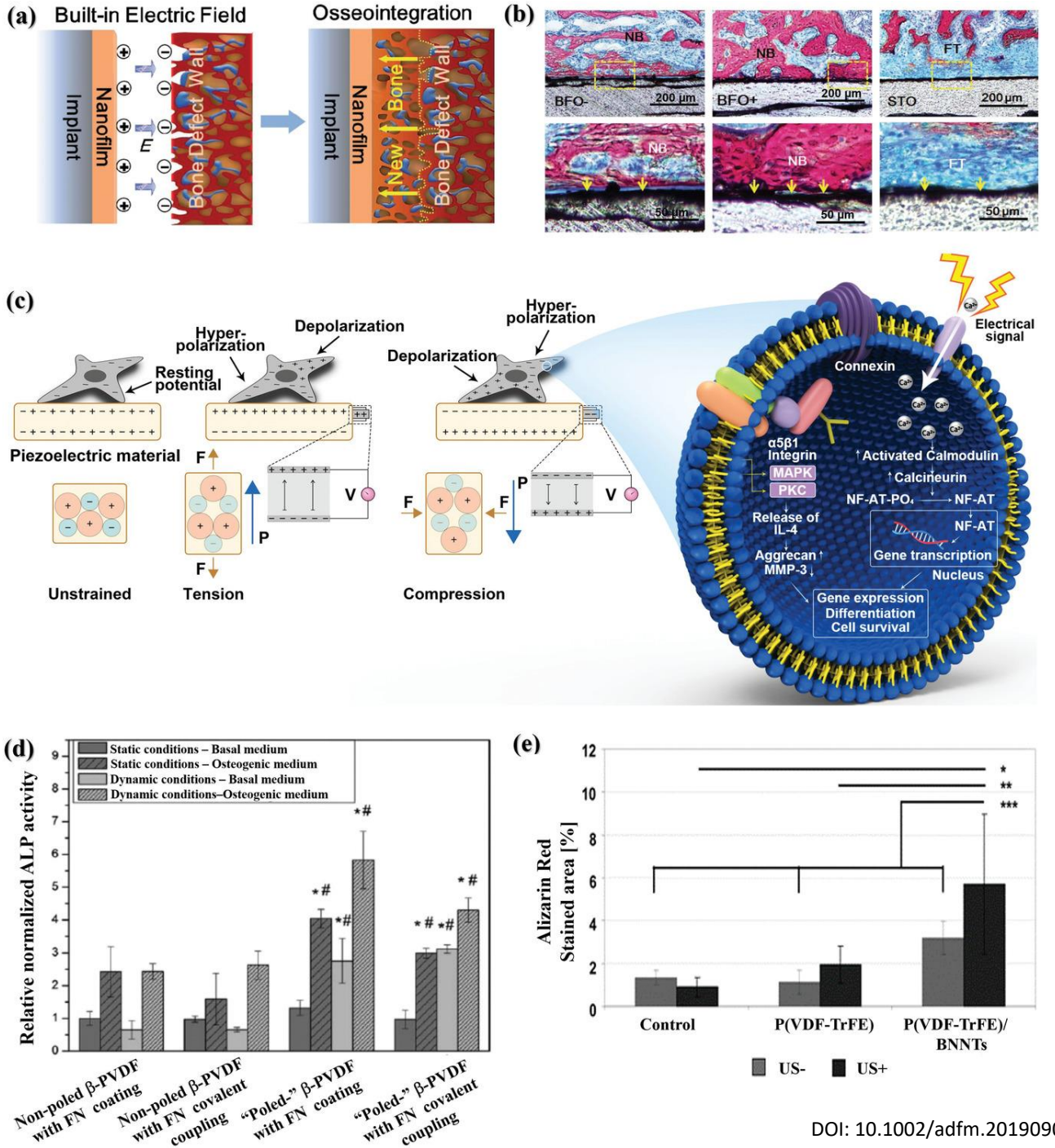

DOI: 10.1002/adfm.201909045

Magnetoelectric 3D scaffolds for enhanced bone cell proliferation

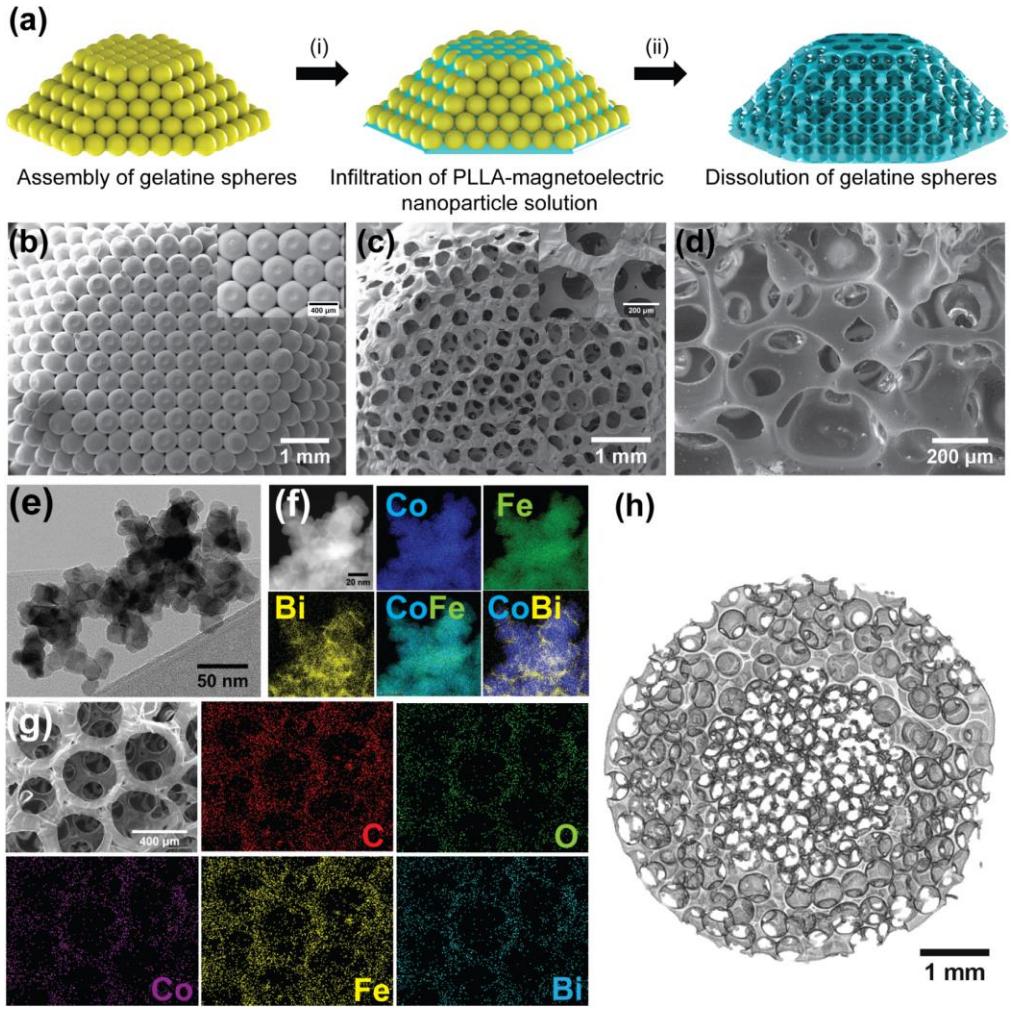

Fabrication of magnetoelectric (ME) inverse opal scaffolds and structural characterization of ME NPs and the ME scaffold. (a) Scheme showing the fabrication stepsstarting with the assembly of gelatin spheres, followed by (i) their infiltration with a solution of PLLA and ME nanoparticles and (ii) the removal of gelatin spheres to obtain3D and porous ME scaffolds. SEM images of (b) assembled gelatin template and the inset show its magnified image. (c) SEM image showing the top-view of a 3D ME scaffoldand the inset shows its magnified image showing a uniform porous structure. (d) SEM image presenting a cross-sectional view of a uniform and well-connected ME scaffold.(e) TEM image showing many overlapped CFO@BFO nanoparticles. (f) HAADF STEM image obtained for some overlapped CFO@BFO nanoparticles and the correspondingEDX maps obtained for Co, Fe and Bi, with the superimposed images clearly showing core–shell CFO@BFO nanoparticles. (g) SEM image obtained for the ME scaffold andthe corresponding EDX maps obtained for C, O, Co, Fe and Bi clearly showing a uniform distribution of ME nanoparticles within the scaffold. (h) Cross-sectional micro-CT 3Dreconstructed image revealing a porosity of 86%.

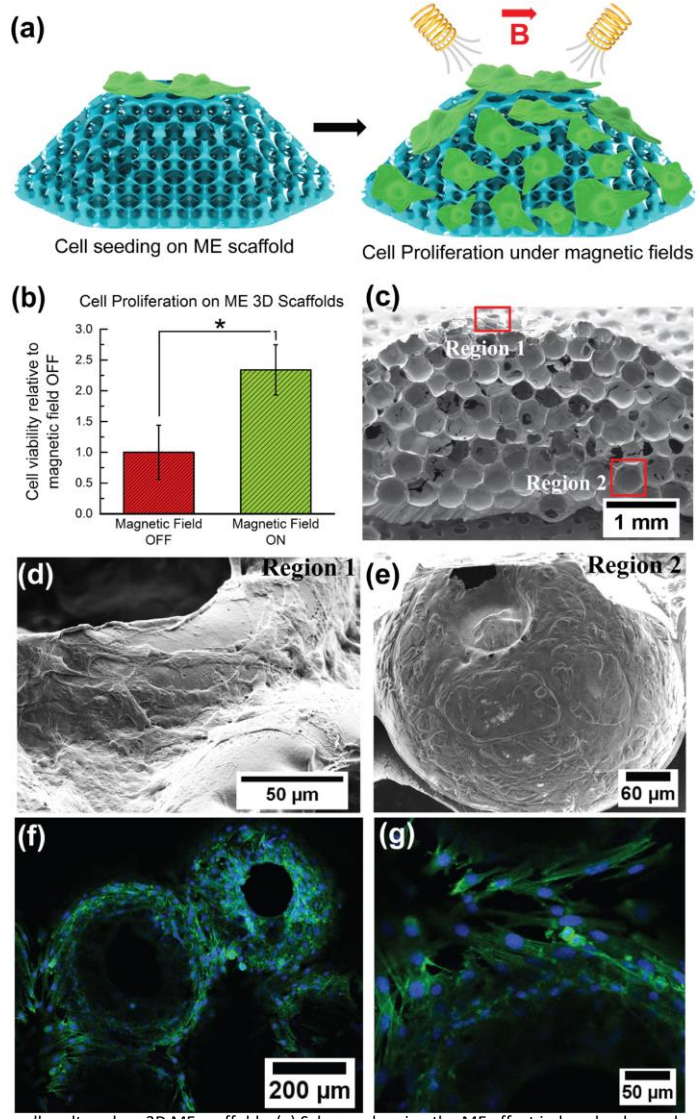

Effect of magnetic stimulation on the cells cultured on 3D ME scaffolds. (a) Scheme showing the ME effect induced enhanced cell proliferation on 3D scaffolds under thei nfluence of AC magnetic fields. (b) Cell viability assay comparing the cell proliferation on 3D ME scaffolds with and without magnetic field stimulation (*p < 0.001). (c) SEMimage showing the cross-section of a 3D ME scaffold seeded with cells and subjected to magnetic fields. Magnified image of the (d) region 1 presents the SEM image taken atthe top of the scaffold from where many attached and interacting cells can be observed. (e) An SEM image taken in region 2 from where the presence of many cells growingon the inside wall of the scaffold can be observed. (f and g) CLSM images of the 3D ME scaffolds with MG63 cells that received magnetic stimulation. Phalloidin-stainedf-actin in green and Hoechst-stained nuclei in blue show an uniformly grown layer of adherent MG63 cells along the curved walls of the scaffold.

Applied Materials Today 16 (2019) 290–300

Bioinspired Three-Dimensional Magnetoactive Scaffolds for Bone Tissue Engineering

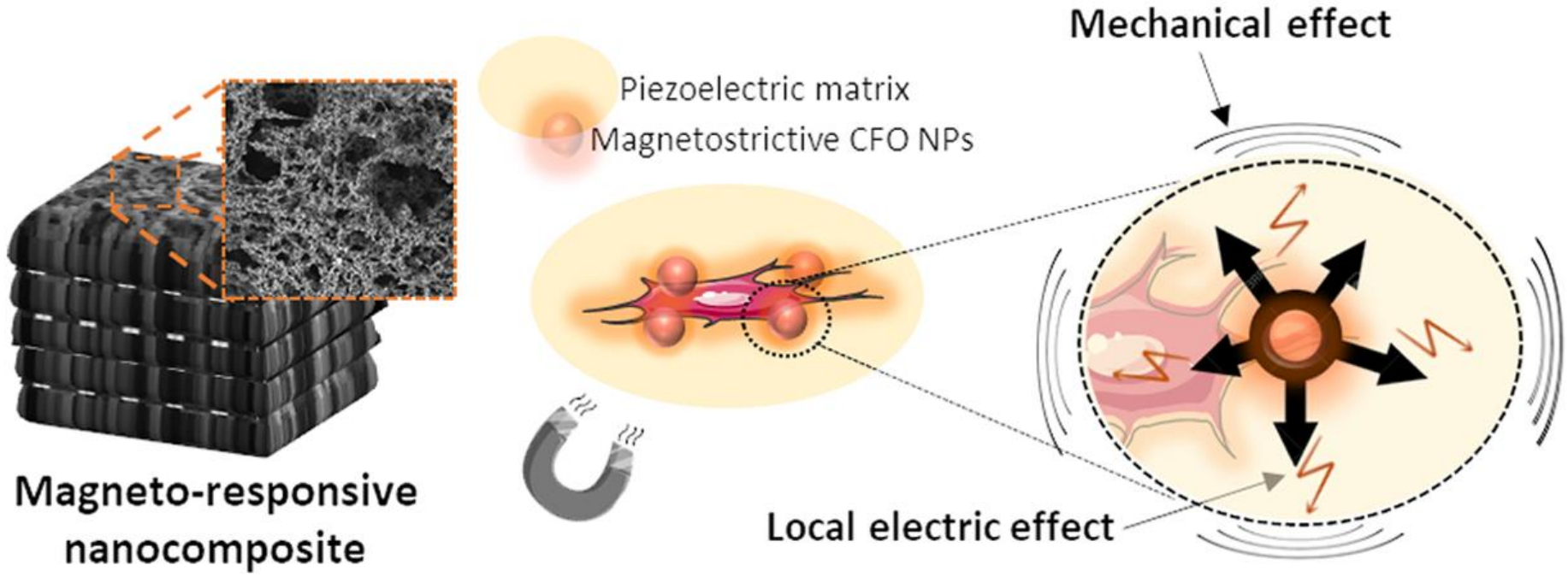

Scaffolds are obtained through the development of nanocomposites comprised of a piezoelectric polymer, poly(vinylidene fluoride) (PVDF), and magnetostrictive particles of $CoFe_2O_4$. Improved proliferation of preosteoblasts through the application of magnetic stimuli is revealed.

This phenomenon is attributed to both local magnetomechanical and magnetoelectric response of the scaffolds, which induce a proper cellular mechano- and electro-transduction process.

ACS Appl. Mater. Interfaces 2019, 11, 45265−45275

Nonresonant powering of injectable nanoelectrodes enables **wireless deep brain stimulation** in freely moving mice

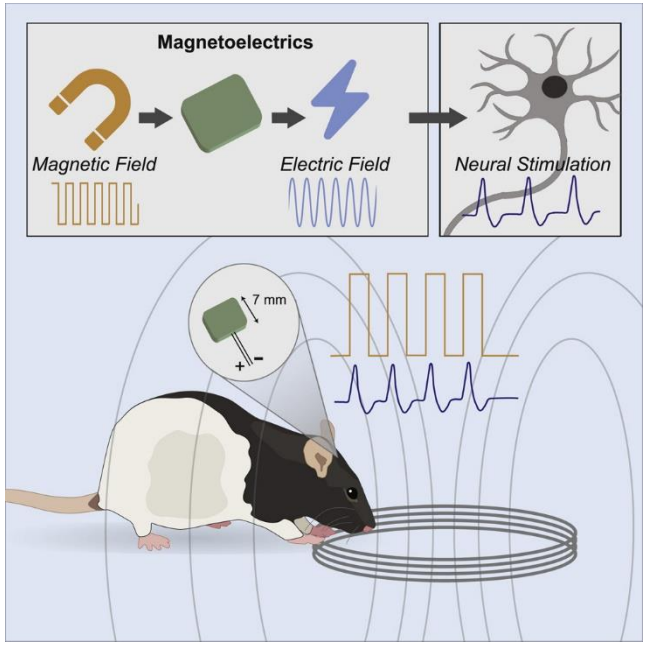

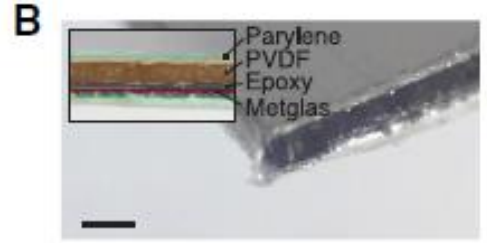

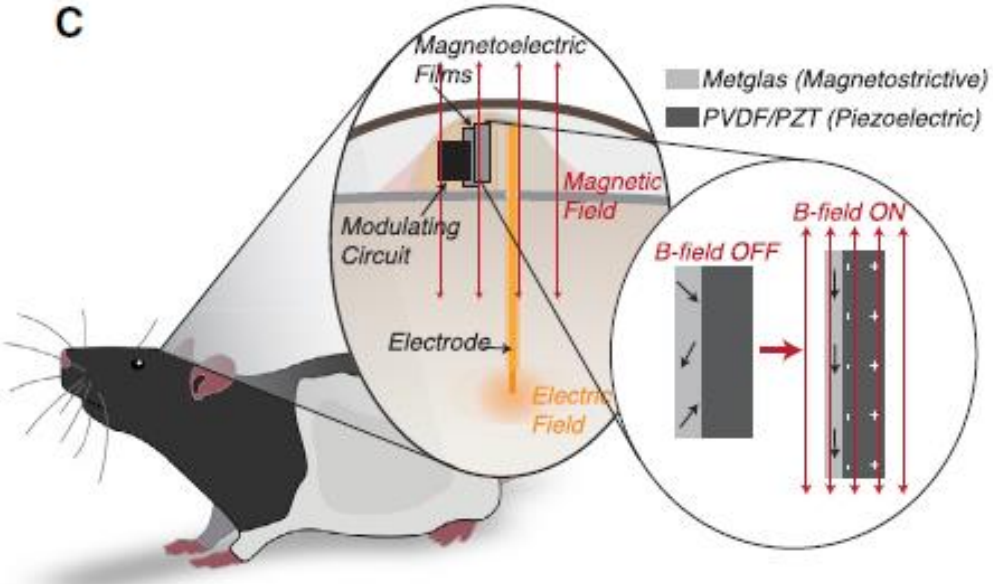

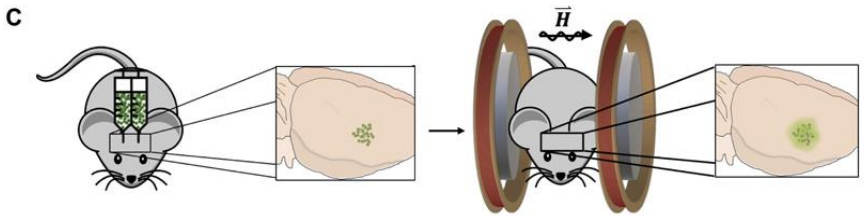

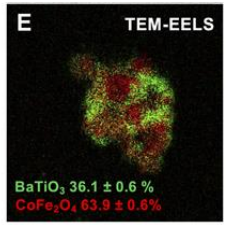

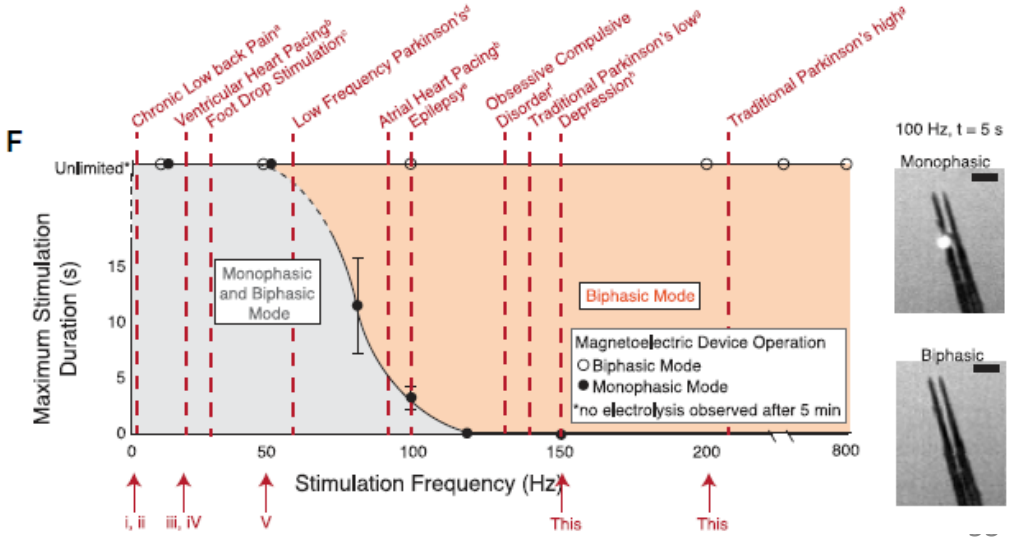

Singer et al., Neuron 107, 631 (202

MagNI: A Magnetoelectrically Powered and Controlled Wireless Neurostimulating Implant

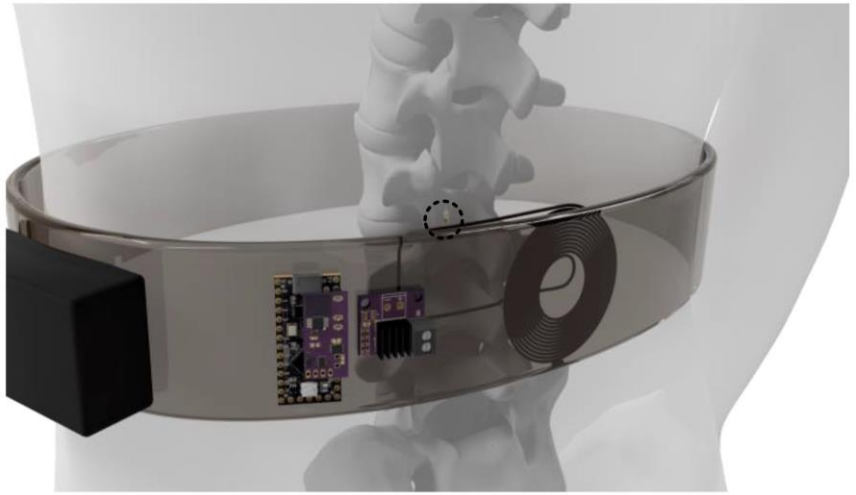

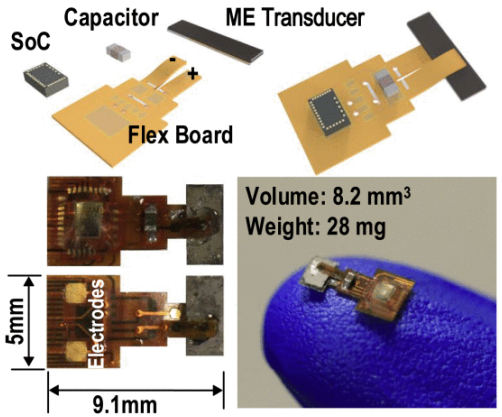

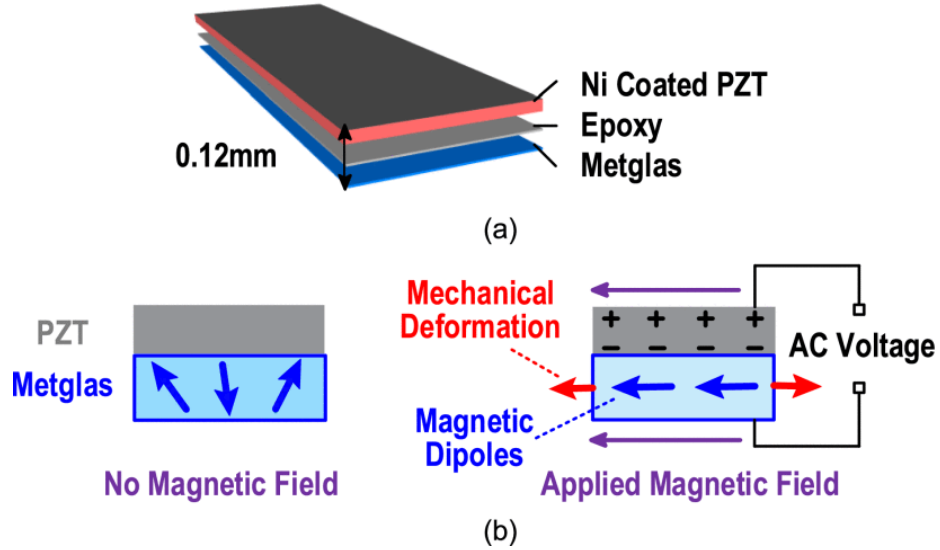

(a) Laminate structure and (b) operating principles of the PZT/Metglasbased magnetoelectric transducer.

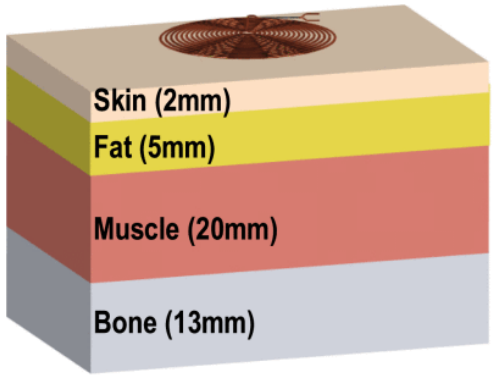

Frequency = 250 kHz

	Relative Permittivity	σ (S/m)	Density (kg/mm^3)
Skin	1100	0.0015	1109
Fat	67.8	0.0436	911
Muscle	576	0.396	1090
Bone	366	0.085	1178

Multilayer human tissue model for safety analysis and material properties of each layer for the EM frequency of 250 kHz.

Wireless and programmable neural stimulator leveraging ME effects for power and data transfer.
ME effect enables safe delivery of high power levels (a few milliwatts) at low resonant frequencies (~250 kHz) to mm-sized implants deep inside the body (30-mm depth).

The system delivers fully-programmable bi-phasic current-controlled stimulation with patterns covering 0.05-to-1.5-mA amplitude, 64-to-512-*μ*s pulse width, and 0-to-200-Hz repetition frequency for neurostimulation.

IEEE TRANSACTIONS ON BIOMEDICAL CIRCUITS AND SYSTEMS, VOL. 14, NO. 6, DECEMBER 2020

Prospective applications of smart materials

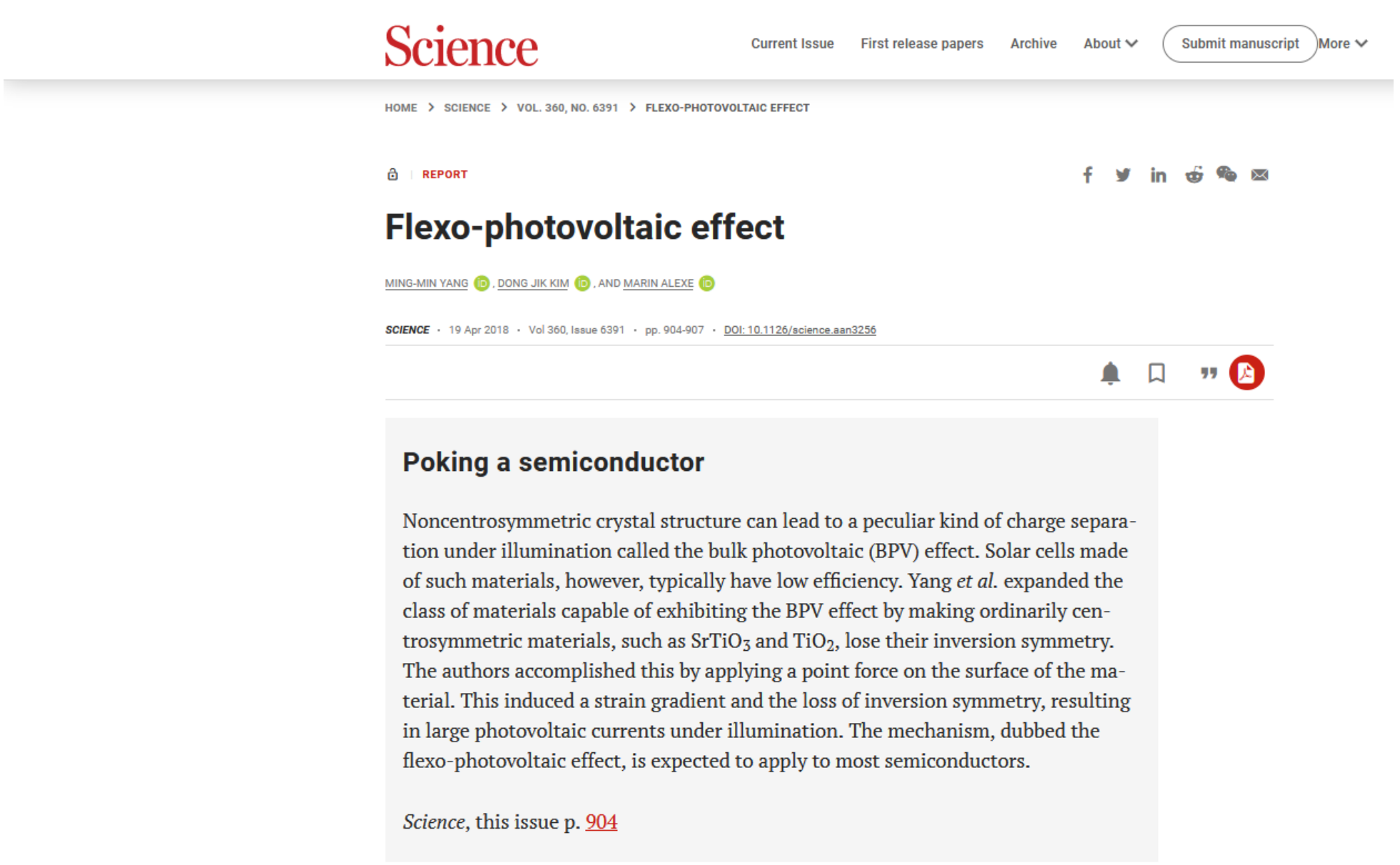

Science

Current Issue First release papers Archive About Submit manuscript More

HOME > SCIENCE > VOL. 360, NO. 6391 > FLEXO-PHOTOVOLTAIC EFFECT

REPORT

Flexo-photovoltaic effect

MING-MIN YANG, DONG JIK KIM, AND MARIN ALEXE

SCIENCE · 19 Apr 2018 · Vol 360, Issue 6391 · pp. 904-907 · DOI: 10.1126/science.aan3256

Poking a semiconductor

Noncentrosymmetric crystal structure can lead to a peculiar kind of charge separation under illumination called the bulk photovoltaic (BPV) effect. Solar cells made of such materials, however, typically have low efficiency. Yang *et al.* expanded the class of materials capable of exhibiting the BPV effect by making ordinarily centrosymmetric materials, such as $SrTiO_3$ and TiO_2, lose their inversion symmetry. The authors accomplished this by applying a point force on the surface of the material. This induced a strain gradient and the loss of inversion symmetry, resulting in large photovoltaic currents under illumination. The mechanism, dubbed the flexo-photovoltaic effect, is expected to apply to most semiconductors.

Science, this issue p. 904

Flexoelectric effect

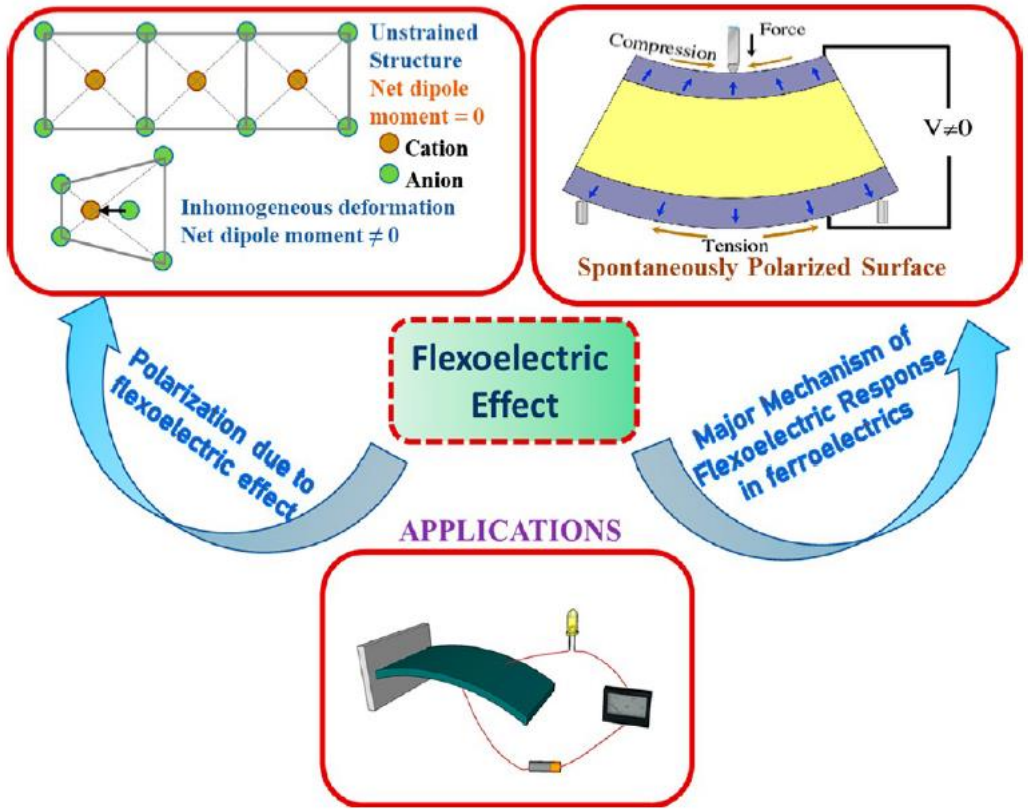

$$P_i \sim d_{ijk}\varepsilon_{jk} + f_{ijkl}\frac{\partial \varepsilon_{jk}}{\partial x_l}$$

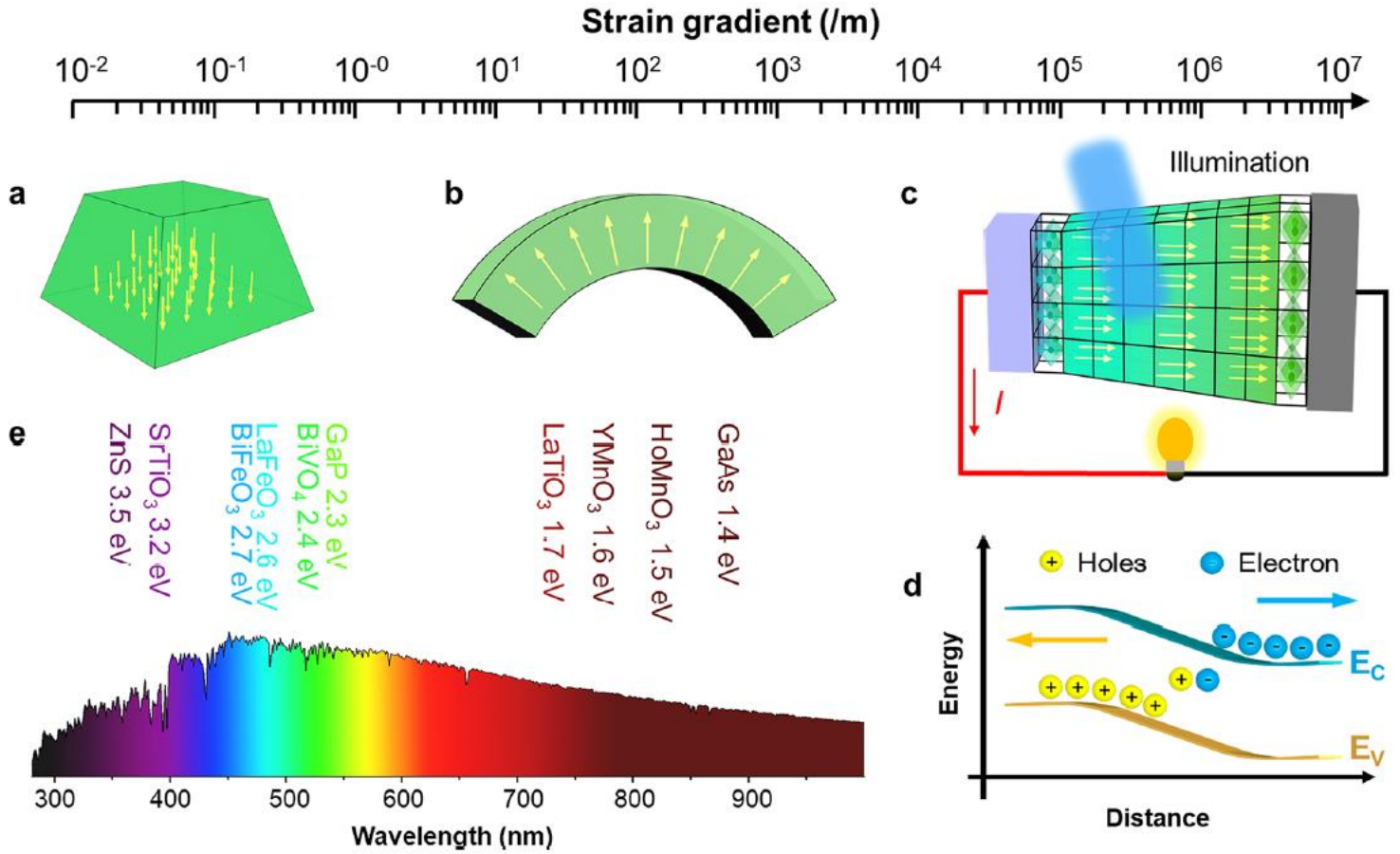

Strain-induced flexoelectric effect

<u>Prospective applications</u>:

- Photovoltaics
- biology (biological membranes, etc)
- chemistry (catalysis, etc.)
- microelectronics (photodiodes and photodetectors, energy harvesting systems for low-voltage devices, etc.)

Nanoscale, 2015, 7, 16555; Nano Lett. 2021, 21, 2946−2952

Thank you very much for you kind attention!